Ground-ice stable isotopes and cryostratigraphy reflect late Quaternary palaeoclimate in the Northeast Siberian Arctic (Oyogos Yar coast, Dmitry Laptev Strait)

Thomas Opel[1,2], Sebastian Wetterich[1], Hanno Meyer[1], Alexander Yu. Dereviagin[3], Margret C. Fuchs[4], and Lutz Schirrmeister[1]

[1] Alfred Wegener Institute Helmholtz Centre for Polar and Marine Research, Periglacial Research Section, Potsdam, 14473, Germany
[2] now at University of Sussex, Department of Geography, Permafrost Laboratory, Brighton, BN1 9RH, United Kingdom
[3] Lomonosov Moscow State University, Geology Department, Moscow, 119992, Russia
[4] Helmholtz-Zentrum Dresden-Rossendorf, Helmholtz Institute Freiberg for Resource Technology, Freiberg, 09599, Germany

Correspondence to: Thomas Opel (thomas.opel@awi.de, t.opel@sussex.ac.uk)

Abstract.

To reconstruct palaeoclimate and palaeonvironmental conditions in the Northeast Siberian Arctic, we studied late Quaternary permafrost deposits at the Oyogos Yar coast (Dmitry Laptev Strait). New infrared stimulated luminescence ages for distinctive floodplain deposits of the Kuchchugui Suite (112.5±9.6 kyr) and thermokarst lake deposits of the Krest Yuryakh Suite (102.4±9.7 kyr), respectively, provide new substantial geochronological data and shed light on the landscape history of the Dmitry Laptev Strait region during the Marine Isotope Stage (MIS) 5. Ground ice stable-isotope data are presented together with cryolithological information for eight cryostratigraphic units and are complemented by data from nearby Bol'shoy Lyakhovsky Island. Our combined record of ice-wedge stable isotopes as proxy for past winter climate conditions covers the last about 200 thousand years and is supplemented by texture-ice stable isotopes which contain annual climate conditions overprinted by freezing processes. Our ice wedge stable-water isotope data indicate substantial variations in Northeast Siberian Arctic winter climate conditions during the late Quaternary, in particular between Glacial and Interglacial but also over the last millennia to decades. Stable isotope values of Ice Complex ice wedges indicate cold to very cold winter temperatures about 200 kyr ago (MIS7), very cold winter conditions about 100 kyr ago (MIS5), very cold to moderate winter conditions between about 60 and 30 kyr ago, and extremely cold winter temperatures during the Last Glacial Maximum (MIS2). Much warmer winter conditions are reflected by extensive thermokarst development during the MIS5c and by Holocene ice-wedge stable-isotopes. Modern ice-wedge stable isotopes are most enriched and testify the recent winter warming in the Arctic. Hence, ice-wedge based reconstructions of changes in winter climate conditions add substantial information to those derived from paleoecological proxies stored in permafrost and allow for distinguishing between seasonal trends of past climate dynamics. Future progress in ice-wedge dating and an improved temporal resolution of ice-wedge derived climate information may help to fully explore the palaeoclimatic potential of ice wedges.

1 Introduction

The wide tundra areas of the Northeast Siberian Arctic lowlands are characterized by deep permafrost deposits that result from cold continental climate conditions in West Beringia during the Late Pliocene and Pleistocene when this region remained non-glaciated (Schirrmeister et al., 2013). The ice-rich permafrost deposits in this area contain huge amounts of

5 ground ice. Syngenetic ice wedges are the major component. Ice wedges are formed by polygonal frost cracking due to thermal ground contraction in winter and the subsequent crack filling in spring (e.g. Leffingwell, 1915; Lachenbruch, 1962). Snow melt is the main source for the water that enters the frost crack, quickly refreezes there due to the negative ground temperatures and forms a vertical ice vein. The periodic repetition of frost cracking and ice-vein formation let ice wedges grow in width and, if synchronous to sedimentation at the surface (syngenetic), also in height.

10 The vertically foliated ice wedges may serve as paleoclimate archives (e.g. Mackay, 1983; Vaikmäe, 1989; Meyer et al., 2002b; Vasil'chuk, 2013), in particular in regions with limited availability of climate archives. They can be studied by means of stable-water isotopes (Dansgaard, 1964). Due to rapid freezing in the frost crack preventing fractionation (Michel, 1982), the isotopic composition of each single ice vein is directly linked to atmospheric precipitation, i.e. winter snow, and, therefore, indicative for the climate conditions during the corresponding cold season. The stable isotope ratios of oxygen

15 (δ^{18}O) and hydrogen (δD) of wedge ice (in ‰ vs. V-SMOW) are related to the condensation temperature of the precipitation and are, therefore, interpreted as proxies for the mean winter air temperature at the study site (Meyer et al., 2015). More negative values reflect colder conditions and less negative values reflect warmer conditions. The d excess ($d=\delta$D-8δ^{18}O) (Dansgaard, 1964) is indicative for the evaporation conditions (i.e. relative humidity, sea surface temperature) in the moisture source region (Merlivat and Jouzel, 1979). In the last years, stable-isotope data from ice wedges have been

20 progressively used to reconstruct past climate changes in Arctic permafrost regions in Northern Siberia (Meyer et al., 2002a; Meyer et al., 2002b; Opel et al., 2011; Wetterich et al., 2011; Vasil'chuk and Vasil'chuk, 2014; Wetterich et al., 2014; Meyer et al., 2015; Streletskaya et al., 2015; Wetterich et al., 2016; Opel et al., in revision) as well as in Alaska (Meyer et al., 2010b; Schirrmeister et al., 2016) and in Canada (Fritz et al., 2012; Porter et al., 2016) on different timescales and with different temporal resolutions.

25 In contrast, intra-sedimental texture ice (pore ice as well as segregated ice lenses and layers) originates from freezing of soil moisture in the seasonally thawed active layer. Soil moisture is fed by varying proportions of different water sources such as summer rain and winter snow as well as melt water of the active layer ice (Mackay, 1983; Vaikmäe, 1989). Additionally, soil moisture is subject to evaporation processes and numerous freeze-thaw cycles before it enters the perennially frozen state. Hence, the stable isotope composition of texture ice has undergone several fractionation processes until the final freezing

30 during permafrost aggradation. It therefore cannot be straightforward interpreted as climate proxy (Wetterich et al., 2014; Wetterich et al., 2016). Nevertheless, the texture-ice isotopic composition has been successfully interpreted in terms of general climate trends such as long-term warming or cooling (Schwamborn et al., 2006; Dereviagin et al., 2013; Porter et al., 2016).

In the Siberian Arctic Laptev Sea region, comprehensive studies of ice-wedge and partly texture-ice stable isotopes of stratigraphic units accessible in coastal exposures have been carried out in the last years at the Mamontova Khayata section of the Bykovsky Peninsula (Meyer et al., 2002a) and at the south coast of Bol'shoy Lyakhovsky Island close to the Zimov'e River mouth (Meyer et al., 2002b). Selected stratigraphic units have been studied at Cape Mamontov Klyk (Boereboom et

5   al., 2013), at Bol'shoy Lyakhovsky Island (Wetterich et al., 2011; Wetterich et al., 2014; Wetterich et al., 2016), at the Oyogos Yar Coast (Opel et al., 2011), and in the Lena River Delta (Schirrmeister et al., 2003b; Wetterich et al., 2008; Schirrmeister et al., 2011a; Meyer et al., 2015). To verify the obtained palaeoclimate results on different timescales and to assess their spatial and temporal representativity, additional extensive ground-ice stable-isotope records are needed.

As for all climate archives, reliable chronologies are crucial for ground-ice based palaeoclimate studies. However, direct

10   dating of ice wedges (Vasil'chuk et al., 2000) is challenging, in particular for the pre-Holocene. Mostly there is only little particulate organic material for radiocarbon dating preserved in ice wedges. Moreover, the ages of late Pleistocene ice wedges are often close to or beyond the age limit of radiocarbon dating. However, new dating tools are in development and comprise radiocarbon dating of air-bubble CO_2 and dissolved organic carbon enclosed ice wedges (Lachniet et al., 2012), Uranium isotopes (Ewing et al., 2015) as well as $^{36}Cl/Cl^-$ dating for Mid- to Late Pleistocene ground ice (Blinov et al., 2009).

15   In many cases, syngenetic ice wedges are therefore only indirectly dated by age determination of the surrounding host sediments. The attribution of host sediments and ice wedges to stratigraphic units with distinct chronological information is often complicated and, hence, regional stratigraphic correlations are challenging (see e.g. discussion in Wetterich et al., 2014).

To address the issue of temporal and spatial representativity of ground-ice stable-isotope records, we present in this paper

20   new data from different Late Quaternary stratigraphic and chronological units at the Oyogos Yar Coast of the Dmitry Laptev Strait. Based on new geochronological and cryolithological information we discuss the cryostratigraphy. We interpret the variability of new ice-wedge and texture-ice stable isotope data and discuss the relevance of ground-ice stable isotopes in terms of paleoclimate and environmental history. We relate our ground-ice stable-isotope data to previously published data from Bol'shoy Lyakhovsky Island in order to generate a Dmitry Laptev Strait ground-ice isotope record and compare it to

25   large-scale climate changes. Furthermore, we shed light on the potential of ice-wedge isotope data as tools for stratigraphic correlations between different study sites.

2 Regional Setting

The Dmitry Laptev Strait connects the Laptev and East Siberian seas (Fig. 1) and its coasts have been subject of geographical and geological research for more than 100 years. The north shore of the Dmitry Laptev Strait, i.e. the south

30   coast of Bol'shoy Lyakhovsky Island represents one of the best-studied Quaternary permafrost sites in Northeast Siberia. Extensive studies of the exposed frozen sediments and ground ice have been carried out to reconstruct environmental dynamics of West Beringia since the mid-Pleistocene (Arkhangelov et al., 1996; Kunitsky, 1996; Meyer et al., 2002b;

Schirrmeister et al., 2002; Andreev et al., 2004; Andreev et al., 2009; Wetterich et al., 2009; Andreev et al., 2011; Schirrmeister et al., 2011b; Wetterich et al., 2011; Tumskoy, 2012; Wetterich et al., 2014; Wetterich et al., 2016 and references therein). In addition, the permafrost exposures of the Oyogos Yar mainland coast at the south shore of the Dmitry Laptev Strait have been studied, but less extensive (Ivanov, 1972; Gravis, 1978; Konishchev and Kolesnikov, 1981; Kaplina
5 and Lozhkin, 1984; Tomirdiaro, 1984; Nagaoka et al., 1995; Wetterich et al., 2009; Kienast et al., 2011; Opel et al., 2011; Schirrmeister et al., 2011b; Rudaya et al., 2015 and references therein).

Stability of permafrost deposits depends basically on climatic conditions during formation, past relief conditions, and the decoupling from seasonal thawing and freezing processes. Warmer interglacial and interstadial periods promote extensive permafrost thaw and subsequent surface subsidence mainly due to ground-ice melt. Such processes termed thermokarst have
10 substantially influenced the study area during the Last Interglacial and since the Lateglacial-Holocene transition. Thawed and refrozen deposits are named as taberite and underlie lacustrine thermokarst deposits (Fig. 2). Due to varying deposition regimes over time as well as temporal and spatial variable patterns of permafrost degradation (and also aggradation) during warm periods, permafrost sequences are often not continuous. This complicates geochronological interpretations as representatives of consecutive late Quaternary periods may be found at laterally different positions and altitudes.

15 Following Tumskoy (2012), permafrost deposits exposed at the Dmitry Laptev Strait span from the MIS7 to the Holocene (Table 1). Yedoma Ice Complex deposits are preserved in sections elevated up to 35 m a.s.l. high while thermokarst basins up to 15 m a.s.l. high exhibit lacustrine and palustrine deposits of the Lateglacial and Holocene periods. Lacustrine deposits of the Krest Yuryakh Suite, which are commonly attributed to the Last Interglacial (Wetterich et al., 2009; Kienast et al., 2011; Tumskoy, 2012) as well as the Buchchagy Ice Complex (MIS 5e-b; Wetterich et al. (2016)) are preserved either below
20 Yedoma Ice Complex or below Lateglacial to Holocene thermokarst deposits (Fig. 2). The stratigraphic position of floodplain deposits attributed to both the Kuchchugui Suite (MIS6; Tumskoy (2012)) and the Zyryanian (MIS4) (Andreev et al., 2004; Andreev et al., 2009) is still under debate.

The main landscape elements, i.e. Yedoma Ice Complex uplands as well thermokarst basins may be cut by thermo-erosional and river valleys and are subject to rapid coastal erosion processes (Günther et al., 2013) that form steep coastal bluffs.
25 Depending on the prevailing type of coastal erosion, thaw slumps may form from Yedoma Ice Complex deposits, shaping a thermo-terrace with thermokarst mounds in front of a steep wall dominated by ice wedges (Fig. 3).

3 Material and Methods

The work presented here is based on material and observations of a one-day reconnaissance trip in 2002 (Schirrmeister et al., 2003a) and a follow-up four-week expedition to the Oyogos Yar coast in 2007 (Schirrmeister et al., 2008) during which
30 about 6 km of the Oyogos Yar coastline were studied between 72.683°N, 143.475°E and 72.672°N, 143.635°E.

3.1 Fieldwork

After overview surveys along the coastal bluffs ice wedges and sediment profiles from all exposed stratigraphic units were selected for extensive investigations and firstly described, photographed and sketched.

After cleaning the exposures from thawed material and debris, horizons were cryolithologically described (French and Shur,

5   2010) and samples were taken by axe and hammer in sub-profiles. The weight of the frozen sample compared to the weight of the sample after oven-drying was used to calculate the gravimetric ice content of the sediments, expressed as weight percentage (wt%) (Van Everdingen, 1998). Values higher than 100 wt% indicate ice over-saturation. Supernatant water from thawed sediment samples was sampled for analysing the stable-water isotope composition of texture ice.

A handheld drilling machine (HILTI TE 5 A) equipped with a core bit was used to obtain frozen sediment cores (150-290

10   cm^3) from profiles Oy7-07 (at 1.5 m asl) and Oy7-08 (at 4.0 m asl) for luminescence dating. Samples were protected from sunlight by using opaque plastic cylinders and sample bags. The sediment of the immediate surroundings of core positions was taken for high-purity Germanium (HPGe) low-level gamma spectrometry of radionuclide concentrations. Subsequent material processing and analyses were performed at the Luminescence Laboratory of the Technical University Bergakademie Freiberg (Germany).

15   In total, we sampled 44 ice wedges from all exposed stratigraphic units, seven in 2002 and 37 in 2007 (Fig. 2). Stable isotope samples from ice wedges were taken by chain saw, by axe or by ice screws along the ice wedge's growth direction (i.e. perpendicular to the frost cracking). The samples were either melted on site with melt water stored in tightly closed 30-ml PE bottles or transported as blocks in frozen state to the cold laboratory of the Alfred Wegener Institute (AWI) in Potsdam for sub-sampling. The melted samples were stored cool (~5°C) before analysing the stable-water isotope composition.

20   Organic material enclosed in ice wedge was picked either in the field or in the AWI cold laboratory for radiocarbon dating.

3.2 Radiocarbon dating

Organic remains enclosed in ice-wedge samples (unidentified plant remains and lemming droppings) as well as plant remains from sediment samples were radiocarbon dated using the accelerator mass spectrometry (AMS) facilities at the Leibniz Laboratory for Radiometric Dating and Stable Isotope Research (Kiel University, Germany) (Grootes et al., 2004),

25   CologneAMS (University of Cologne, Germany) (Dewald et al., 2013; Rethemeyer et al., 2013) and Poznań Radiocarbon Laboratory (Adam Mickiewicz University, Poznań, Poland) (Goslar et al., 2004). Conventional ^{14}C ages were calculated according to (Stuiver and Polach, 1977). Calibrated ages were determined as yr b2k (before CE2000) using Oxcal 4.2 (Bronk Ramsey, 2009) based on the IntCal13 dataset (Reimer et al., 2013).

3.3 IRSL dating

30   The cores were processed for quartz and feldspar at target grain size fractions of 20-40 μm, 40-63 μm, 63-100 μm, and 90-160 μm. Lacking coarse-grained material (>100 μm) and quartz optically stimulated luminescence (OSL) signals close to

saturation required focusing on feldspar infrared stimulated luminescence (IRSL) of the grain size fraction 63-100 μm. Carbonates and organics were removed using 10% HCl and 30% H_2O_2, respectively. Feldspar flotation (0.2% HF, pH 2.4-2.7, dodecylamine) removed the quartz from sample extracts and subsequent density separation enriched K-feldspars (2.53-2.58 g cm^{-3}). Etching (10% HF, 5 min) removed the outer 10-μm layer of individual grains.

5 Aliquots of 2 and 1 mm diameter reflect the trade-off between low grain number per aliquot (reduced averaging of inter-grain variations) and sufficient luminescence signal intensities. The IRSL signals of feldspars were measured using a TL/OSL DA-20 Reader (Bøtter-Jensen et al., 2003) equipped with a ^{90}Sr beta irradiation source (4.95 Gy min^{-1}).

Signals were stimulated at 870 nm (IR diodes, 125 °C for 100 s) and detected through a 410 nm optical interference filter (Krbetschek et al., 1997). The measurement sequence followed the single-aliquot regenerative-dose (SAR) protocol

10 according to Murray and Wintle (2000), including cycles to record recycling ratios, recuperation, and correct for sensitivity changes. Appropriate measurement conditions were evaluated and adjusted based on preheat tests and dose-recovery tests (Murray and Wintle, 2003). Processing of measured data and statistical analyses were performed using the software Analyst v4.31.7 (Duller, 2015) and the R package 'Luminescence' (Kreutzer et al., 2012), version 0.6.4. The small data set (n = 5) restricted age modelling to a simple measure of central tendency, i.e. arithmetic mean. The large data set (n = 49) showed no

15 evidence for insufficient bleaching due to low scatter (standard deviation below 10%) and low skewness (<0.5) of equivalent doses and hence, suggested paleodose calculation based on the central age model (CAM) (Galbraith et al., 1999). Final IRSL ages, including dose rate modelling, were estimated using the software ADELE (Kulig, 2005). For the determination of the mineral-internal dose rate of the K-feldspars, a potassium content of 12.5 ± 0.5% was assumed (Huntley and Baril, 1997).

3.4 Stable-isotope analysis

20 Using a mass spectrometer (Finnigan 215 MAT Delta-S) equilibrium technique was applied to analyse the oxygen (δ^{18}O) and hydrogen (δD) stable-isotope ratios of all ice-wedge and texture-ice samples in the stable isotope laboratory of AWI Potsdam. The values are given in delta per mil notation (δ, ‰) relative to the Vienna Standard Mean Ocean Water (VSMOW) Standard. Based on long-term standard measurements, the reproducibility of 1σ is better than ±0.1‰ for δ^{18}O and ±0.8‰ for δD, respectively (Meyer et al., 2000). The deuterium excess d (Dansgaard, 1964) was calculated by $d=\delta$D-

25 $8\delta^{18}$O.

For this study, we considered only ice wedges with a clear stratigraphic relation to one of the studied units and at least three samples. Exceptions were made only for a small Holocene ice wedge at the top of the Yedoma Ice Complex (two samples) as well as for narrow modern ice wedges, i.e. single veins or groups of ice veins representing the youngest ice-wedge growth stage (one to two samples). Following this, from the 44 sampled ice wedges, we considered in the following only 28. Partly,

30 ice-wedge data were only interpreted as groups (i.e. recent ice wedge parts and modern ice veins).

In several cases, stable-isotope data, preferentially those from samples at the edge of ice wedges showed clear signs of post-genetic fractionation processes owing to exchange processes between wedge ice and surrounding sediments. The respective

data are characterized by distinctly elevated $\delta^{18}O$ and δD values and decreased d excess values and were excluded from further analysis and interpretation.

Similar to ice wedges, we considered only texture-ice stable-isotope data with a clear attribution to one of the studied units and only units with at least three data points.

4 Results

Within this paper, we focus on our extensive studies of cryostratigraphy and, in particular, ground-ice stable isotopes. For more detailed results and discussion of distinct sediment profiles we refer to Wetterich et al. (2009), Schirrmeister et al. (2011b) and Wetterich et al. (2016). From these papers we also adopted most radiocarbon ages derived from sediment samples.

4.1 Stratigraphy, cryolithology and geochronology

Eight cryolithological units were distinguished during fieldwork at the Oyogos Yar coast (Table 1, Fig. 2). The studied ice wedges were attributed to five of the units based on field observations.

4.1.1 Unit I

The oldest unit studied at the Oyogos Yar coast is represented by floodplain deposits related to the **Kuchchugui Suite**, which typically shows a subdivision into two horizons. The lower one consists of brownish-grey laminated silty sands and is characterized by a relatively low ice content (31-53 wt%) with massive cryostructure and peat inclusions as well as thin in-situ grass roots. The upper horizon is built from more ice-rich (up to 140 wt%) silty sands with bended, belt-like and lens-like reticulate cryostructures. It also contains grass roots and peat inclusions and is covered by a dark-brown peat soil layer.

Syngenetic ice wedges in these deposits are rather small and can be found in two ways. The first type consists of 0.3 to 0.75 m wide composite wedges (sand-ice wedges) composed of alternating ice and sand veins (1 to 10 mm wide). They exhibit rounded truncated heads and are buried by the upper sediment horizon of unit I. The second type is represented by intersecting multistage ice wedges, i.e. composite wedges that upwards pass over into regular ice wedges of 0.5 to 1 m width. Their clean, transparent ice shows many vertically oriented air bubbles (1-5 mm in diameter) and pronounced ice veins of 3-6 mm thickness. Additionally, epigenetic ice wedges from the overlying unit II penetrate into the Kuchchugui deposits.

Radiocarbon dating of moss peat from the upper horizon directly above composite wedge Oya IW1 revealed a non-finite age of >44.5 cal kyr b2k for the leached residue and a mean age of 45.2 cal kyr b2k for humic acid, respectively (Table 3).

IRSL analyses of feldspars (63-100 μm, n = 49, CAM) yielded a deposition age of 112.5±9.6 kyr for sample Oy7-07-01. Suitable IRSL signal properties are indicated by high signal intensity, good reproducibility and low recuperation. This is

confirmed by a low coefficient of variation in doses recovery tests (6.7%). The low standard deviation and low skewness value indicate no bleaching issues (Table 2) and suggest a reliable IRSL age estimation.

4.1.2 Unit II

Unit II represents the **Buchchagy Ice Complex**. It is characterized by two distinct peat horizons up to 1 m thick about 3 m

5   apart (Wetterich et al., 2016). The corresponding sediments are relatively ice-rich (gravimetric ice content 61-112 wt%, except for the peat horizons with even higher values), brown to grey silty sands with peat inclusions as well as lens-like and layered cryostructures. Unit II contains syngenetic ice wedges 2 to 4 m wide and several m deep that penetrate into unit I. Partly they are truncated and buried below grey loam with many peat inclusions, likely representing the lower peat horizon. The wedge ice of rather dirty yellowish-grey colour exhibits numeral mineral inclusions and air bubbles of 1-5 mm in

10   diameter. Ice-vein thickness is about 3-5 mm.

The only dating results available are infinite radiocarbon ages (>51 kyr BP and >49 kyr BP; Table 3) for the two distinctive peat layers (Wetterich et al., 2016). At the southern coast of Bol'shoy Lyakhovsky Island, opposite to the Oyogos Yar coast, the respective peat horizons of the Buchchagy Ice Complex show infinite radiocarbon ages as well, whereas radioisotope (^{230}Th/U) disequilibria dating revealed ages of 126+16/-13 and 118+19-14 kyr for the lower, and 93±5 and 89±5 for the

15   upper peat horizon (Wetterich et al., 2016). This geochronological information can be transferred to the Oyogos Yar coast. The chronostratigraphic link is supported by ice-wedge stable isotope data (see chapter 5.2).

4.1.3 Unit III

Unit III refers to deposits of the **Krest Yuryakh Suite** that is commonly related to the Last Interglacial. This unit comprises two different kinds of deposits, both associated to thermokarst lake development. The first type likely represents a

20   succession of an ancient lake margin. It consists of dark grey to grey brown silts with mollusc shells as well as plant detritus layers and plant inclusions, partly accompanied by wood fragments. The cryostructure is lens-like reticulated in the upper part and coarse lens-like reticulated in the lower part. The gravimetric ice content is low (20 to 40 wt%). The second type represents lacustrine sediments filling ice-wedge casts above grey taberal deposits with massive cryostructure. They consist of grey clayish sandy silts with brown peat lenses and alternating plant detritus layers, characterized by a lens-like reticulated

25   to layered cryostructure and single ice lenses. The upper part shows decreasing plant detritus content and numerous mollusc shells. No syngenetic ice wedges were found.

A mean radiocarbon age of 48.3 cal kyr b2k was obtained from leached residue of wood in sample Oya-3-11 from an ice-wedge cast (Table 3).

IRSL analyses of sample Oy7-08-25 could only be based on few aliquots (n = 5) due to the limited material in the suitable

30   grain size fraction (63-100µm). Nevertheless, the low coefficient of variation (6.3%) in dose recovery tests (n = 5) indicates appropriate luminescence properties and measurement conditions. Reliable feldspar properties are further supported by high

signal intensity, good reproducibility, low standard deviation and low skewness (Table_2). The IRSL results date unit III to 102.4±9.7 kyr.

4.1.4 Unit IV

Unit IV represents the **Yedoma Ice Complex** that constitutes of grey-brown sandy silts with small peat lenses and larger peat inclusions, which originate from buried cryosols, as well as twig fragments, grass roots and fine distributed plant detritus. The cryostructure is determined layered and lens-like reticulated between ice bands. The gravimetric ice content ranges from 50 to more than 200 wt%. Huge syngenetic ice wedges up to 8-10 m wide in the higher sections (2-5 m in the lower sections) reach heights of more than 20 m. The wedge ice is mostly dirty grey as typical for Yedoma Ice Complex ice wedges with varying sediment contents but partly also milky white, indicating a much higher number of small air bubbles. Vertically oriented ice veins are mostly between 1 and 5 mm wide.

According to mean radiocarbon ages the **Yedoma Ice Complex** was deposited in the time period between about 49.4 and 36.3 cal kyr b2k (Table 3). Several age reversals have been found; hence no clear age-depth relationship could be established.

4.1.5 Unit V

In the vast thermokarst basin, unit V consists of **taberal Yedoma Ice Complex deposits**, which thawed during thermokarst formation below a lake and refroze after lake drainage or desiccation. Unit V is represented by light-grey silts with lens-like layered cryostructure and very little plant detritus. The gravimetric ice content is around 40 wt%. Unit V is completed by a paleosol layer with twigs and peat inclusions. No syngenetic ice wedges were found.

Radiocarbon ages of taberal Yedoma Ice Complex deposits revealed mean ages of about 46.0 and 40.1 cal kyr b2k (Table 3) and confirm the period of Yedoma Ice Complex deposition.

4.1.6 Unit VI

The Late Glacial to Holocene sequence starts with **lacustrine deposits** of unit VI with lens-like layered cryostructure, partly filling ice-wedge casts. The gravimetric ice content is 40 to 70 wt%. Unit VI is characterised by alternating layers of silty fine sand and plan detritus and contains also wood fragments and mollusc shells. The lake deposits are covered by a 20 to 30 cm thick peat horizon. No syngenetic ice wedges were found.

Radiocarbon dating revealed a Late Glacial age (means about 18.1 to 12.7 cal kyr b2k) of the thermokarst-lake deposits (Table 3).

4.1.7 Unit VII

The **palustrine deposits** of unit VII consist of ice-rich greyish sandy silts, partly containing peat lenses. The cryostructure is layered and coarse lens-like reticulated. The gravimetric ice content is 13 to 180 wt%. The recent polygonal surface of the

thermokarst basin is mirrored by widely distributed and actively growing syngenetic ice wedges. They are up to 3.5 m wide and up to about 8 m high with toes that reach down until the taberal deposits of unit V. Their ice is mostly transparent to milky white but sometimes also dirty grey due to higher density of sediments and organic matter. Single ice veins are 1 to 10 mm wide. The ice of the most recent ice wedge parts as well as of the up to 8 cm wide and up to 20 cm high modern rejuvenation stages is more milky white due to a higher number of small air bubbles.

The palustrine deposits in the thermokarst basin accumulated over the Holocene (about 11.5 to 3.6 cal kyr b2k) with the pronounced peat horizon dated to about 9.3 cal kyr b2k (Table 3). Organic remains in ice-wedge samples indicate syngenetic ice-wedge growth over the Late Holocene, i.e. since about 2.0 cal kyr b2k (Table 4).

4.1.8 Unit VIII

Unit VIII depicts the up to 1-2 m thick **Holocene cover** on top of the Yedoma Ice Complex. Unit VIII was only found in places and associated with initial thermokarst. The deposits are characterised by brownish grey loam with numerous peat inclusions and a layered cryostructure. The gravimetric ice content is 54 to 118 wt%. Small, milky white syngenetic ice wedges less than 1 m wide penetrate into the Yedoma Ice Complex ice wedges. Moreover, Holocene cracking activity characterised by milky white ice veins was also observed in the upper parts of the huge ice wedges of the Yedoma Ice Complex.

The Holocene cover deposits were radiocarbon dated to the early Holocene with mean ages of about 11.0 to 8.9 cal kyr b2k (Table 3).

4.1.9 Generalised stratigraphic sequences

The described cryolithological units and the respective ice wedges have been studied in three **generalised stratigraphic sequences** A to C (Fig. 2).

The first sequence A represents the stratigraphic situation of the eastern part of the study area (A in Fig. 2). It consists of Kuchchugui floodplain deposits of unit I, Buchchagy Ice Complex (unit II), and Krest Yuryakh thermokarst lake deposits (unit III), discordantly overlain by Yedoma Ice Complex (unit IV) and Holocene cover (unit VIII).

The second sequence B in the central part of the study area (B in Fig. 2) comprises in the lower part Kuchchugui floodplain deposits (unit I) covered by Buchchagy Ice Complex (unit II) and Krest Yuryakh thermokarst lake deposits (unit III). The main part consists of Yedoma Ice Complex deposits (unit IV) overlain by the Holocene cover (unit VIII).

Sequence C in the western part of the study area (C in Fig. 2) are represented by about 10 m high thermokarst basin outcrops and comprise Krest Yuryakh thermokarst lake deposits (unit III), covered by taberal Yedoma Ice Complex (unit V) as well as Late Glacial to Holocene thermokarst lake (unit VI) and palustrine deposits (unit VII).

4.2 Stable isotope composition of ground ice

The studied ice wedges of different units as well as their basic parameters and stable-isotope data are presented in Table 5. The attribution of ice wedges to certain stratigraphic units is based on field observations and stable-water isotope data. Additionally, texture-ice stable isotope data are summarised in Table 5. Overall, both ice-wedge and texture-ice stable-

5 isotope data show a high variability over time.

4.2.1 Unit I Kuchchugui floodplain deposits

The composite wedges exhibit mean $\delta^{18}O$ values of -30.7‰ for Oya IW1 (δD: -240.5‰) and -28.2‰ for Oy7-03 IW4 (δD: -225.6‰), respectively, with low internal variability (Fig. 4, Table 5). Their respective mean d excess values were low (4.8% and 0‰). The corresponding slopes (intercepts) in a $\delta^{18}O$-δD bi-plot are 7.41 and 6.7 (-13.23 and -36.78), respectively.

10 The intersected multi-stage ice wedges showed in the composite-wedge parts (Oy7-03 IW1+5) mean values of -29.7‰ for $\delta^{18}O$, -235.0‰ for δD, and 2.3‰ for d excess with a regression line of $\delta D=8.68*\delta^{18}O+22.46$ ($r^2=0.98$). The upper regular part showed the lowest $\delta^{18}O$ and δD mean values (-34.1‰ and -268.0‰, respectively) observed in all units at the Oyogos Yar Coast (Fig. 4, Table 5). The mean d excess value is 4.9‰ and the co-isotopic regression line $\delta D = 8.74*\delta^{18}O +29.99$ ($r^2=0.93$).

15 Texture-ice stable-isotope values scatter between -29.8‰ and -23.1‰ for $\delta^{18}O$, -231.8‰ and -191.4‰ for δD, as well as -8.0‰ and 6.2‰ for d excess (Fig. 4, Table 5). The regression line in a co-isotopic $\delta^{18}O$-δD plot is $\delta D=6.24*\delta^{18}O-48.31$ ($r^2=0.99$), quite similar to that of composite wedge Oy7-03 IW4.

4.2.2 Unit II Buchchagy Ice Complex deposits

One syngenetic ice wedge was attributed to the Buchchagy Ice Complex (Oy7-07 IW1). The mean stable water isotope

20 values (n=7) are -33.1‰ for $\delta^{18}O$, -258.3‰ for δD, and 6.7‰ or d excess with very little variability (Fig. 4, Table 5). The regression line in a $\delta^{18}O$-δD bi-plot is $\delta D=6.96*\delta^{18}O-27.89$ ($r^2=0.98$).

Texture-ice stable-isotope values scatter between -29.8‰ and -23.3‰ for $\delta^{18}O$, -233.8‰ and -184.9‰ for δD, and -1.9‰ and 9.9‰ for d excess (Fig. 4, Table 5). The regression line in a co-isotopic $\delta^{18}O$-δD plot with $\delta D=6.89*\delta^{18}O-26.83$ ($r^2=0.98$) is similar to the ice-wedge data.

25 #### 4.2.3 Unit IV Yedoma Ice Complex deposits

In total, ten ice wedges of the Yedoma Ice Complex were studied in different altitude levels from 1.5 to about 35 m a.s.l. In places, in particular close to the ground surface at the top of the Ice Complex as well as at the slope to the thermokarst basin, the ice wedges showed evidence of Holocene frost-cracking activity. The respective samples, i.e. those with $\delta^{18}O$ values higher than -28.0‰ (maximum value of unaffected ice wedges of unit IV and slightly lower than the minimum value (-

30 27.1‰) of Holocene ice wedges in unit VII), were accordingly attributed to unit VIII (Holocene cover deposits).

The overall mean stable isotope values of the Yedoma Ice Complex ice wedges are -30.8‰ for $\delta^{18}O$, -240.2‰ for δD, and 5.9‰ for d excess with a regression line of $\delta D=8.33*\delta^{18}O+15.92$ ($r^2=0.98$). The mean values for single ice-wedge profiles vary between -32.8‰ and -29.2‰ for $\delta^{18}O$, -258.3‰ and -227.6‰ for δD, and 3.7‰ and 8.1‰ for d excess (Fig. 4, Table 5) without any clear altitudinal trend (Fig. 5).

5   The texture-ice stable-isotope values exhibit an enormous scatter and vary between -34.5‰ and -18.5‰ for $\delta^{18}O$, -253.9‰ and -150.5‰ for δD, and -10.9‰ and 21.7‰ for d excess (Fig. 4, Table 5). The co-isotopic regression line is $\delta D=6.51*\delta^{18}O-36.00$ ($r^2=0.97$). A substantial altitudinal variability shows a generally decreasing (increasing) trend in $\delta^{18}O$ and δD (d excess) values from about 6 m a.s.l. to a pronounced minimum (maximum) around 20 m a.s.l. and again higher (lower) values above (Fig. 5).

10   **4.2.4 Unit VII Palustrine deposits**

The ice-wedge stable-isotope samples from unit VII can be attributed to four groups: (1) older lower sections, (2) high-resolution vertical profiles in the younger upper section, (3) recent, i.e. central parts of upper sections and (4) modern ice veins, i.e. rejuvenation stages. The first two groups show quite similar isotopic compositions with mean values between -25.4‰ and -25.0 ‰ for $\delta^{18}O$, -194.6‰ and -192.0‰ for δD, and 7.5‰ and 8.8‰ for d excess with co-isotopic slopes

15   between 7.53 and 7.67 and intercepts between -3.76 and -0.75 (Fig. 4, Table 5). The recent ice wedge parts exhibit more enriched isotopic compositions with mean values of -22.7‰ for $\delta^{18}O$, -173.9‰ for δD, as well as 7.6‰ for d excess, whereas the modern ice veins show the most enriched mean values of all samples: -20.7 ‰ for $\delta^{18}O$, -158.3‰ for δD, and 7.7‰ for d excess. The co-isotopic regression lines are with $\delta D=8.03*\delta^{18}O+8.33$ ($r^2=0.99$) and $\delta D=7.79*\delta^{18}O+3.23$ ($r^2=0.99$), respectively, close to the Global Meteoric Water Line (GMWL: $\delta D=8*\delta^{18}O+10$).

20   The texture-ice stable-isotope values group between -21.9‰ and -16.0‰ for $\delta^{18}O$, -171.4‰ and -124.2‰ for δD, and -3.7‰ and 10.7‰ for d excess (Table 5) $\delta^{18}O$ and δD build two clusters in the co-isotope plot (Fig. 4). The regression line is close to that of the ice wedges ($\delta D=7.57*\delta^{18}O-6.35$) but with a weaker correlation ($r^2=0.88$).

4.2.5 Unit VIII Holocene cover on top of the Ice Complex

The Holocene-influenced ice-wedge parts of the Yedoma Ice Complex show relative little isotope variations. Mean values

25   vary between -26.7‰ and -25.9 ‰ for $\delta^{18}O$, -205.1‰ and -200.2‰ for δD, as well as 6.7‰ and 8.4‰ for d excess. The co-isotopic regression slopes vary between 8.47 and 9.22 with intercepts between 18.81 and 40.26 (Fig. 4, Table 5). The two samples from a small ice wedge in the initial thermokarst depression shows slightly more enriched values (mean $\delta^{18}O$: -24.9‰, mean δD: -195.6‰, mean d excess: 10.1‰).

The texture-ice stable-isotope data are more enriched and spread between -20.7‰ and -17.6‰ for $\delta^{18}O$, -157.1‰ and -

30   134.2‰ for δD, as well as 6.6‰ and 10.4‰ for d excess. The regression line accounts for $\delta D=7.23*\delta^{18}O-7.02$ ($r^2=0.99$).

5 Discussion

5.1 Chronostratigraphy and landscape development of the Oyogos Yar mainland

We identified eight cryostratigraphic units at the Oyogos Yar coast, four less than at the opposite southern coast of Bol'shoy Lyakhovsky Island (Table 1). They represent basically three main landscape types which have undergone different

5 permafrost aggradation and degradation patterns that varied over time and in space: Ice Complex deposits, flood plain deposits and thermokarst basin deposits. Hence, often a clear attribution of deposits and ice wedges to distinct units and their relation to each other is challenging, in particular for pre-Yedoma Ice Complex units which cannot be dated by the radiocarbon method.

At the Oyogos Yar coast we did not find deposits of the Yukagir Ice Complex (^{230}Th/U dated to 200.9±3.4 kyr) and the

10 Zimov'e layer (IRSL-dated to 134±22 kyr) both known from Bol'shoy Lyakhovsky Island (Table 1). Hence, at our study site Kuchchugui floodplain deposits represent the oldest unit (unit I). The obtained IRSL age of 112.5±9.6 kyr of unit I in sequence B (Fig. 2) is older by about 10 kyr than the respective ages of Kuchchugui deposits from Bol'shoy Lyakhovsky Island, but falls within the error range of the previous age determinations (Table 1). The latter were obtained from Kuchchugui taberal deposits below an ice-wedge cast attributed to the Last Interglacial. Hence, they may be influenced by

15 thaw and refreeze during subsequent thermokarst lake development and may therefore represent rather minimum ages (Andreev et al., 2004).

The radiocarbon ages of >44.5 and 45.2 cal kyr b2k point to a much younger age of unit I in the eastern sequence A (Fig. 2) but are close to the limit of the radiocarbon method. The stratigraphic position of unit I below deposits of the Buchchagy Ice Complex of unit II supports the age information obtained from IRSL dating which is why we discard the radiocarbon age.

20 However, to exclude a possible attribution of unit I in the eastern part of the study region to the Zyryanian Stadial known from Bol'shoy Lyakhovsky Island (Table 1) additional age control is highly needed, if possible also using other approaches, e.g. uranium decay series in ground ice (Ewing et al., 2015). The Zyryanian at Bol'shoy Lyakhovsky Island shows similar sedimentary characteristics pointing to floodplain deposits (Andreev et al., 2004), but contains toes of Yedoma Ice Complex ice wedges instead of small truncated composite wedges found for unit I at Oyogos Yar. Kuchchugui ice wedges of unit I at

25 Oyogos Yar are smaller and do not exhibit so depleted isotope values as compared to Bol'shoy Lyakhovsky Island (see section 5.2). The ^{36}Cl/Cl$^-$ ages of 98±31 and 68±31 kyr (Blinov et al., 2009) for ice wedges Oy7-03 IW1 and IW2 cannot finally resolve the attribution to a genetic unit but rather confirm the IRSL age for unit I in section A. We therefore, interpret unit I in section A as floodplain deposits of the early MIS5 with subsequent Ice Complex formation.

The Buchchagy Ice Complex (unit II) is known from both sides of the Dmitry Laptev Strait and represents Ice Complex

30 formation of MIS5 age. It developed above the Kuchchugui floodplain deposits from 126+16/-13 kyr and 117+19/-14 kyr to 93±5 kyr and 89±5 kyr as deduced by ^{230}Th/U dating of two enclosing peat horizons on Bol'shoy Lyakhovsky Island (Wetterich et al., 2016). Its syngenetic ice wedges penetrate into the underlying Kuchchugui floodplain deposits. Given the

age of the Kuchchugui deposits and the rather large uncertainty range of the ^{230}Th/U dating (in particular for the lower peat), the Buchchagy Ice Complex development likely took place in MIS5d-5b between about 110 and 90 kyr. The cryostratigraphic relation of unit II of Oyogos Yar to Bol'shoy Lyakhovsky Island is additionally confirmed by the very similar stable-isotope composition of ice-wedge samples from both locations (see section 5.2; Fig. 6).

5   The Krest Yuryakh lacustrine and palustrine thermokarst deposits (unit III) indicate warm temperatures, at least in the summer season. They have been formed in ice-wedge casts and wide thermokarst basins within degraded ice-rich Buchchagy Ice Complex of unit II and are therefore younger. In this paper we present the first direct age determination for the Krest Yuryakh Suite at the Dmitry Laptev Strait derived from deposits within an ice-wedge cast. The IRSL age of 102.4±9.7 kyr points to an origin of unit III rather during the MIS5c than during MIS5e (Eemian) as previously associated (Wetterich et al.,

10   2009; Kienast et al., 2011). This, however, fits good to a maximum in modeled summer temperatures around 105 kyr b2k (Andreev et al., 2011; Ganopolski and Calov, 2011) (Fig. 7). It further narrows the duration of Buchchagy Ice Complex development. The radiocarbon age of about 48 cal kyr b2k again obtained at the very limit of the radiocarbon method might point to a distinctly younger formation of unit III. However, as it clearly contradicts the IRSL age, we assume relocation of the dated material and therefore, discard this age. Given the dating uncertainties and temporal overlaps for units I to III an

15   absolute chronology is still challenging. Moreover, a temporal coexistence of Ice Complex accumulation plains, thermokarst basins and floodplains in the same region during MIS5 seems to be possible.

In contrast to Bol'shoy Lyakhovsky Island, there is neither dating nor sedimentary evidence for floodplains of the Zyryanian stadial (MIS4) at Oyogos Yar (Table 1), even though a presence in the eastern section A cannot be ruled out and asks for age control as part of future studies.

20   Starting from at least 50 kyrs b2k Yedoma Ice Complex (unit IV) formed at Oyogos Yar, confirming earlier findings (Gravis, 1978; Kaplina and Lozhkin, 1984; Tomirdiaro, 1984; Nagaoka et al., 1995). Radiocarbon ages from Bol'shoy Lyakhovsky Island indicate even earlier Ice Complex formation since about 60 cal kyr b2k (Table 1; Wetterich et al., 2014). Even though the youngest age from unit IV is dated to 36.3 cal kyr b2k (Table 4) a longer development can be assumed as indicated from Bol'shoy Lyakhovsky Island where ages of 33.5 to 32.5 cal kyr 2bk have been found for the Molotkov

25   interstadial stratum of the Yedoma Ice Complex (Table 1; Andreev et al., 2009; Wetterich et al., 2014). It remains unclear whether the development of the Yedoma Ice Complex at Oyogos Yar has further continued or the accumulation regime has changed. On Bol'shoy Lyakhovsky Island the prevailing Yedoma Ice Complex formation moved from plain to erosional landforms such as river valleys where the Sartan stadial stratum of the Yedoma Ice Complex has been formed at least between about 30 and 26.7 cal kyr b2k (Wetterich et al., 2011). At Oyogos Yar potential equivalent Ice Complex deposits in

30   river valleys have not been found along the studied coastline section but may exist further east in the vicinity of the Kondrat'eva River.

Consequently it is not possible to estimate whether there has been substantial permafrost degradation on the top of the Oyogos Yar Ice Complex during the postglacial warming as well as the duration of the potential erosional gap. The

Holocene cover (unit VIII) has been developed since 11 cal kyr b2k according to our data that mirror Bol'shoy Lyakhovsky Island conditions (Andreev et al., 2009; Wetterich et al., 2014).

Dated taberal Ice Complex deposits of unit V and the overlying lacustrine deposits of units VI and VII prove widespread permafrost degradation related to the development of vast thermokarst basins during the last deglaciation. Thermokarst

5   started at Oyogos Yar around 18 cal kyr b2k; about 3 kyr earlier than reported from Bol'shoy Lyakhovsky Island (Andreev et al., 2009; Wetterich et al., 2009). The lacustrine phase (unit VI) of the studied Oyogos Yar thermokarst basin development ended around 13 cal kyr b2k and was followed by the palustrine phase (unit VIII) continuing until today. This confirms results of earlier studies (Gravis, 1978; Kaplina and Lozhkin, 1984; Tomirdiaro, 1984; Nagaoka et al., 1995). In contrast, on Bol'shoy Lyakhovsky Island the lacustrine phase of the studied thermokarst basins ended only around 8 cal kyr b2k

10   (Andreev et al., 2009; Wetterich et al., 2009). However, thermokarst development depends on manifold factors as such as (micro-)climate, relief, substrate, ice content, and drainage. Hence, these deviations are regarded as minor given the fact that they fit into the general temporal pattern of thermokarst formation during the last deglaciation (Walter et al., 2007).

A predominantly lateral ice-wedge growth in the last two millennia can be concluded from radiocarbon ages of actively growing ice wedges of unit VII (Table 4) indicating rather stable surfaces in the thermokarst basins with low accumulation.

15   **5.2 Regional palaeoclimate deduced from ground ice and its stable-isotope compositions**

For all Oyogos Yar units the stable-water isotope compositions of ice wedges are more depleted than those of texture ice. Mean δ^{18}O values of ice wedges are between about 2‰ and 8‰ and mean δD values between about 15‰ and 58‰ lower than the corresponding mean values of texture ice (Fig. 4). Except for two ice wedges of unit VIII mean ice-wedge d excess values are higher by about 1‰ to 7‰ than the respective values of texture ice. The slopes in a δ^{18}O-δD diagram are in most

20   cases lower for texture ice than for ice wedges (Table 5). This reflects the differences in ice genesis involving different water sources and fractionation processes. Whereas ice-wedge stable isotopes reflect a direct winter climate signal, in particular the contribution of summer precipitation as well as evaporation effects may be responsible for the more enriched stable isotope values of texture ice (Meyer et al., 2002a; Schwamborn et al., 2006). On the other hand, freezing processes within the seasonally thawed active layer would both enrich and deplete stable-isotope values as discussed below. Hence, it can be

25   concluded that texture-ice stable isotopes rather reflect secondary fractionation processes than climate information. However, mean texture-ice stable-isotope data may indicate generally colder climate conditions for the formation of units I, II and IV during distinct periods of the last Interglacial and Glacial and significantly warmer conditions for the formation of units VII and VIII during the Holocene.

The enormous scatter of texture-ice stable isotopes within the Yedoma Ice Complex (unit IV) leads to the interpretation that

30   it does reflect mainly secondary fractionation processes rather than climate conditions. In particular the δ^{18}O and δD minimum with corresponding d excess maximum around 20 m a.s.l., where texture ice δ^{18}O and δD values drop even below ice wedge δ^{18}O and δD values, indicates massive not climate-related secondary fractionation processes (Fig. 5). Besides changing proportions of different moisture sources (summer and winter precipitation, melt water) and evaporation from

active layer and polygonal ponds, in particular numerous freeze-thaw cycles with moisture segregation are assumed to control the soil moisture's stable-isotope composition before it enters a perennially frozen state. During freezing of soil moisture the first ice exhibits a heavier isotopic composition than the remaining and in particular the last moisture and ice. Hence, the $\delta^{18}O$ and δD decrease from 15 to 21 m a.s.l. is most likely related to persistent sediment freezing from below

5   leading to very low isotope values in the last freezing stage.

In contrast, more detailed and constrained climate variability is traceable from ice-wedge stable-isotope values, in particular when a reliable age control is available. This is indicated by ice-wedge co-isotopic slopes closer to the GMWL (Table 5) and recent precipitation (Meyer et al., 2002b; Opel et al., 2011). Ice-wedge stable isotopes allow to detect winter temperature variability on different time scales from Glacial-Interglacial scale over intra-unit scale (such as within unit IV Yedoma Ice

10   Complex) up to centennial scale (such as within an ice wedge). However, on the long-term scale ice wedges provide rather snapshots of past climate conditions whereas they may provide centennial-scales time series on according millennial time-scales (Opel et al., in revision).

In the following we discuss the ice-wedge stable-isotope data from Oyogos Yar obtained within this study. In a first step we relate our data to those from Bol'shoy Lyakhovsky Island published earlier (Meyer et al., 2002b; Wetterich et al., 2009;

15   Wetterich et al., 2011; Wetterich et al., 2014; Wetterich et al., 2016) to enhance the palaeoclimatic understanding for the entire Dmitry Laptev Strait region (Fig. 6). However, one has to keep in mind that apart from few ice wedges in units IV (only Bol'shoy Lyakhovsky) and VII (Oyogos Yar and Bol'shoy Lyakhovsky) all ice wedges are dated only indirectly by age determinations of host sediments. Due to the downward transfer of snowmelt and corresponding stable isotope signatures into the several meters deep frost cracks, ice wedges are always younger than host sediments at the exactly same

20   altitude. It is so far not possible to determine the age offsets for different units but depending on deposition rates estimated age offsets of a few hundreds to few thousands years seem to be most reasonable to us.

The oldest ice wedges at the Dmitry Laptev Strait are from the Yukagir Ice Complex on Bol'shoy Lyakhovsky Island, dated to 200.9±3.4 kyr (Table 1). The formation of Ice Complex ice wedges point to stable climate and accumulation conditions. (Meyer et al., 2002b) reported according mean stable-isotope values of around -32‰ for $\delta^{18}O$ and around -250‰ for δD

25   (Fig. 6). The inferred cold to very cold winter climate conditions indicate strong seasonal differences for the late MIS7 with warm and wet summers as reconstructed from biological proxies in host sediments (Andreev et al., 2004).

The occurrence of composite wedges in Kuchchugui floodplain deposits (unit I) at Oyogos Yar points to rather dry winter conditions that provided not enough snow to fill the frost cracks by snowmelt and/or a high accumulation regime that delivers sufficient material (e.g. wind-blown sand) to cause the high sediment fraction in these composite wedges. The latter

30   is supported by the fact that the studied composite wedges (Oy7-03 IW4 and Oya IW1) are buried and truncated. Their rounded thaw surfaces indicate a deepening of the active layer or a local water body that leads to a melting of the composite wedges surface before deposition of new sediments. Their mean $\delta^{18}O$ (-28.2‰ and -30.7‰) and δD (-227‰ and -244‰) values point to moderate to cold winter temperatures during formation. However, given the little widths of the composite wedges and their high sediment content, the low internal variability, low d excess values and low slopes may indicate

different levels of isotopic exchanges between ice veins, sediment veins and host sediments (Meyer et al., 2002a; Meyer et al., 2010a). This is in particular likely for Oy7-03 IW4, which additionally shows a co-isotopic regression similar to that of corresponding texture ice (Table 5). Hence, we exclude the composite-wedge data from our palaeoclimatic interpretation. Interestingly, composite wedges Oy7-03 IW1+5 show similar regression lines as the intersected ice wedges Oy7-03 IW1+2

5   they pass into, but with distinctly enriched mean isotope values (δ^{18}O: -29.7‰, δD: -235‰ compared to δ^{18}O: -34.1‰, δD: -268‰, respectively). Whereas the first fits well into the described composite-wedge pattern the latter represent the minimum isotope values found at Oyogos Yar and indicate very cold winter climate for the initiation of ice-wedge genesis in the Kuchchugui unit I.

Even severe climate conditions can be inferred from two Kuchchugui ice wedges on Bol'shoy Lyakhovsky Island. Mean

10   stable isotope values of about -35.5‰ for δ^{18}O and -280‰ for δD -235‰ (Fig. 6) indicate extremely cold winter temperatures (Meyer et al., 2002b). As pollen-based reconstructions point to relative cold summer temperatures (Andreev et al., 2011) generally cold climate conditions can be concluded for this period, attributed to the MIS5 stadial.

The presence of the Buchchagy Ice Complex (unit II) indicates cold-stage climate conditions during its formation on both sides of the Dmitry Laptev Strait. Very cold and stable winter climate conditions during ice-wedge formation are confirmed

15   by ice-wedge δ^{18}O and δD values (means -33‰ and -258‰, respectively), which are slightly lower than those of the Yukagir ice wedges. The isotopic composition is nearly identical on both sides of the Dmitry Laptev Strait (Fig. 6) and underlines the stratigraphic correlation. Pollen-based reconstructions from host sediments indicate cool summer temperatures (Wetterich et al., 2016) and clearly point to stadial conditions with a generally colder climate in MIS5d.

The thick deposits of the Yedoma Ice Complex (unit IV) with their huge ice wedges mirror long-term cold stage conditions

20   during the MIS3 (Molotkov interstadial stratum) from about 60 cal kyr b2k to about 32 cal kyr b2k. Mean δ^{18}O and δD values of -31‰ and -240‰, respectively, generally confirm cold winter temperatures during ice-wedge formation, but slightly warmer than those of Yukagir and Buchchagy ice wedges (Fig. 6). The variability of stable-isotope values with respect to altitude indicates changing conditions from very cold to moderate winter temperatures. Similar variations have been observed in corresponding Yedoma Ice Complex ice wedges from Bol'shoy Lyakhovsky Island (Meyer et al., 2002b;

25   Wetterich et al., 2014). However, due to age reversals in the dated sediment profiles (Fig. 5; Schirrmeister et al., 2011b) it is not possible to attribute single ice-wedge profiles to distinct time periods. It is noteworthy that the ice-wedge profiles close to the top of unit IV exhibit more depleted isotope compositions likely pointing to climate deterioration towards the transitions to MIS2.

The Sartan stadial stratum of the Yedoma Ice Complex on Bol'shoy Lyakhovsky Island formed at least between about 30

30   and 26.7 cal kyr b2k (Table 1) and exhibits the lowest stable-isotope values (mean δ^{18}O of -37‰, mean δD of -290‰) (Fig. 6) found in ice wedges of the Dmitry Laptev Strait. They indicate extremely cold winter temperatures during the Last Glacial Maximum. A generally cold climate is furthermore confirmed by pollen-based temperature reconstruction from the host sediments (Wetterich et al., 2011).

Significantly enriched stable-isotope values were found in Holocene Oyogos Yar ice wedges in both cover deposits of the Yedoma Ice Complex (unit VIII) and palustrine sediments of thermokarst basins (unit VII) (Fig. 6). Mean δ^{18}O (δD) values of about -26‰ (-200‰) and -25‰ (-190‰), respectively, point to warm interglacial winter temperatures during ice-wedge formation. Similar mean values (δ^{18}O: -24.5‰, δD: -187‰) could be obtained from corresponding ice wedges on Bol'shoy

5   Lyakhovsky Island (Meyer et al., 2002b; Wetterich et al., 2009). Distinctly warmer summer temperatures were also derived from pollen-based reconstructions that, however, indicate a gradual cooling since the Early Holocene (Andreev et al., 2009). The warming from the Last Glacial to the Holocene is also accompanied by a slight increase (about 2‰ for Oyogos Yar, about 1‰ for Bol'shoy Lyakhovsky Island) in mean *d* excess values (Table 5). This likely indicates only minor changes in the moisture generation and transport patterns and/or seasonality of precipitation between Pleistocene and Holocene.

10   Whereas there exist no dating results for ice wedges from the cover deposits, radiocarbon ages from ice wedges of palustrine thermokarst deposits on both sides of the Dmitry Laptev Strait indicate that the derived temperature information can be attributed mainly to the last two millennia. It is even possible to go more into detail. The recent parts of actively growing ice wedges at Oyogos Yar exhibit more enriched mean δ^{18}O (δD) values of about -23‰ (175‰). The highest δ^{18}O (δD) values of about -20.5‰ (160‰) on Oyogos Yar and Bol'shoy Lyakhovsky Island (Meyer et al., 2002b) were determined for

15   modern ice veins, i.e. the youngest, actively growing ice-wedge rejuvenation stages. They represent the warmest winter temperatures mirrored in ice-wedge stable isotopes from the Dmitry Laptev Strait (Fig. 6).

5.3 Relation of ice-wedge palaeoclimate information to large-scale climate dynamics

The present ice-wedge stable-isotope record of the Dmitry Laptev Strait is based on new data from Oyogos Yar and earlier data from Bol'shoy Lyakhovsky Island. It contains ice-wedge isotopes from seven stratigraphic units and covers roughly 200

20   kyr (Table 1, Fig. 6). Other regional ice-wedge based reconstructions such as those from Cape Mamontov Klyk (Boereboom et al., 2013), the Lena River Delta (Wetterich et al., 2008), Bykovsky Peninsula (Meyer et al., 2002a) or Duvanny Yar at the Kolyma River (Vasil'chuk et al., 2001) date only back to MIS3 or MIS4 and/or contain only single stratigraphic units (Streletskaya et al., 2015). Therefore, we additionally compare our data to the continuous NGRIP ice-core δ^{18}O record from Greenland (North Greenland Ice Core Project members, 2004) with age scale GICC05modelext (Wolff et al., 2010) as well

25   as climate-model output (Fig. 7). For the latter we use mean summer (JJA) and (extended) winter (DJFMAM, the cold period of the year, likely covered by ice wedges) temperatures for the Laptev Sea region (centred at about 70°N, 120°E) from the Earth System model of intermediate complexity CLIMBER-2 (Petoukhov et al., 2000) driven by orbital forcing and greenhouse gas concentrations (Ganopolski and Calov, 2011).

The inferred cold to very cold temperature of Yukagir Ice Complex ice wedges (age about 200 kyrs b2k) do not fit to the

30   modelled winter temperatures of this period, in contrast to warm summer temperatures inferred from pollen. Considering an age offset between ice wedges and the dated peat horizon it is likely that the ice wedges are younger and correspond to decreasing modelled winter temperatures between 200 and 180 kyrs b2k (Fig. 7).

The very cold to extreme cold temperatures reflected in stable isotopes of Kuchchugui ice wedges dated to about 110 to 100 kyr b2k do not fit the modelled winter temperatures, but a minimum in winter insolation around 100 kyr b2k (Laskar et al., 2004) (not shown). Modelled cold winter periods were either earlier (around 130 kyr b2k) or later (around 90 kyr b2k) both accompanied by cold summer temperatures (Fig. 7) as also inferred from Kuchchugui pollen (Andreev et al., 2011). In

5 contrast, the NGRIP ice-core record shows a colder period around 110 kyr b2k that might correspond to the very low ice-wedge δ^{18}O and δD values of the Kuchchugui ice wedges in unit I. Considering a potential Zyranian age interpretation for the according floodplain deposits in sequence A (see section 5.1), even the very cold MIS4 stadial (around 65 kyr b2k) seems to be possible interpretation.

The inferred very cold winter temperatures of the Buchchagy Ice Complex ice wedges do not correspond to an according

10 cold period in modelled winter temperatures as well but may fit to the cold period around 110 kyr b2k seen in the NGRIP ice core. A younger age can be ruled out as the Krest Yuryakh warm period with enhanced thermokarst processes including melting of ice wedges attributed to the Buchagy Ice Complex is centred about 102 kyr b2k (MIS5c).

All in all, or data show a rather unexpected climate variability during the MIS5. Surprisingly cold winter conditions during MIS5d were succeeded by the peak interglacial warming during MIS5c leading to widespread thermokarst formation with

15 vast thermokarst lakes.

Both, the NGRIP ice core record and the modelled temperatures (summer and winter) show high-frequency climate fluctuations during the MIS3. Even though not temporally resolvable, the altitudinal variability in ice-wedge isotopes at Oyogos Yar (Fig. 5) and Bol'shoy Lyakhovsky indicates that similar climate variations likely have affected the Dmitry Laptev Strait region as well. Similar fluctuations within the same range of δ^{18}O and δD values have also been reported for

20 Cape Mamontov Klyk (Boereboom et al., 2013), the Bykovsky Peninsula (Meyer et al., 2002a), and Duvanny Yar (Vasil'chuk et al., 2001). A more stable MIS3 summer climate, even though with a distinct interstadial optimum around 40 cal kyr b2k was inferred from pollen data onfrom Bol'shoy Lyakhovsky and other study sites in the Laptev Sea region (Wetterich et al., 2014).

The extremely cold winter temperatures reflected by ice-wedges stable isotopes of the Sartan stadial Yedoma Ice Complex

25 on Bol'shoy Lyakhovsky correspond well to the Last Glacial Maximum cold period in the NGRIP ice core record and the modelled temperatures (Fig. 7). Interestingly, such extremely depleted δ^{18}O and δD values have not been found at any other study site in the Laptev Sea region, even though corresponding Ice Complex strata have been studied extensively (Wetterich et al., 2011).

The substantial warming from the Last Glacial to the Holocene as captured by modelled temperatures and the NGRIP record

30 is also found in our Dmitry Laptev Strait record as well as other regional ice-wedge stable-isotope records such as Cape Mamontov Klyk (Boereboom et al., 2013), Lena River Delta (Wetterich et al., 2008), and Bykovsky Peninsula (Meyer et al., 2002a). The detected δ^{18}O difference of about 6‰ between the studied Yedoma Ice Complex and Holocene ice wedges corresponds well to the regional pattern. However, if compared to the Last Glacial Maximum the winter warming at the Dmitry Laptev Strait was about twice as much, underlining the peculiarity of this cold event.

The slightly increasing mean *d* excess values which go along with the Last Glacial to Holocene transition are in line with observations at Cape Mamontov Klyk (Boereboom et al., 2013) and in the Lena River Delta (Wetterich et al., 2008) and indicate rather constant moisture generation and transport pathways over this transition. In contrast, mean *d* excess values at the Bykovsky Peninsula show an increase of about 10‰ (Meyer et al., 2002a) pointing to substantial changes in the local to
5 regional moisture regime.

The NGRIP record as well as the modelled summer temperatures show a cooling after the Northern Hemisphere Early Holocene insolation maximum. In contrast, our ice-wedge data and the modelled winter temperatures verify a general Holocene winter warming trend with the highest temperatures today (Fig. 7) which is likely related to seasonal insolation and greenhouse gas forcing (Meyer et al., 2015).

10 **6 Conclusions and outlook**

The present study summarises comprehensive stable- isotope data from ice wedges interpreted as winter climate proxy from the Oyogos Yar mainland coast in addition and in comparison to pre-existing data from Bol'shoy Lyakhovsky Island in the Northeast Siberian Arctic covering the last about 200 kyr. Seven distinct generations of ice-wedge development are distinguished, confirming coldest winter climate conditions during MIS5 and MIS2, warmest conditions during MIS1 and
15 winter climate instability during MIS3. Since dating ice wedges directly is challenging and chronostratigraphic correlation to surrounding frozen deposits holds difficulties, which are even more complicated by different dating approaches beyond the radiocarbon limit (such as luminescence dating and radioisotope disequilibria dating), further method development is needed in ice-wedge dating and in understanding of the chronological relation between ice wedges and host sediments (i.e. age offsets). However, in course of the present study valuable geochronological data was obtained by IRSL dating of deposits of
20 the Kuchchugui stratum to MIS5d (112.5±9.6 kyr) and of deposits of the Krest Yuryakh stratum to MIS5c (102.4±9.7 kyr), formerly assigned with the MIS5e. If comparing ice-wedge stable isotope data to climate model output (CLIMBER-2) and Greenland ice core records (NGRIP) high correspondence was found for MIS2 and MIS1. For older periods it is more difficult due to dating issues and rather low temporal resolution. In particular, high and rapid climate variability during MIS5 present in three units in the Oyogos Yar record holds controversial potential and asks for further research to improve the
25 application of ice wedge stable isotopes as winter climate proxy.

Author contributions

TO initiated and designed the present study, and wrote the paper with contributions of the other co-authors. TO, AD, HM, SW, and LS sampled and described ground ice and sediments. HM carried out stable-isotope analyses and helped with interpretation. MF conducted IRSL dating and provided interpretation. SW and LS provided stratigraphic information and
30 interpretation. All co-authors contributed to the final discussion of obtained results and interpretations, and have approved the final version of the manuscript.

Acknowledgements

The study presented here is part of the Russian-German System Laptev Sea cooperative scientific effort. We thank our colleagues who helped during fieldwork and following discussions as well as the staff of the AWI Potsdam stable isotope laboratory. We thank Andrey Ganopolski (PIK Potsdam, Germany) for providing climate model output. Markus Richter (TU Dresden, Germany) and Ingrid Stein (TU Bergakademie Freiberg, Germany) supported IRSL dating. This study contributes to the project "Ice wedges as winter climate archives – towards high-quality chronologies, advanced process understanding and new paleoclimate records" (Deutsche Forschungsgemeinschaft grant no. OP217/3-1).

References

Andreev, A. A., Grosse, G., Schirrmeister, L., Kuzmina, S. A., Novenko, E. Y., Bobrov, A. A., Tarasov, P. E., Ilyashuk, B. P., Kuznetsova, T. V., Krbetschek, M., Meyer, H., and Kunitsky, V. V.: Late Saalian and Eemian palaeoenvironmental history of the Bol'shoy Lyakhovsky Island (Laptev Sea Region, Arctic Siberia), Boreas, 33, 319-348, 10.1080/03009480410001974, 2004.

Andreev, A. A., Grosse, G., Schirrmeister, L., Kuznetsova, T. V., Kuzmina, S. A., Bobrov, A. A., Tarasov, P. E., Novenko, E. Y., Meyer, H., Derevyagin, A. Y., Kienast, F., Bryantseva, A., and Kunitsky, V. V.: Weichselian and Holocene palaeoenvironmental history of the Bol'shoy Lyakhovsky Island, New Siberian Archipelago, Arctic Siberia, Boreas, 38, 72-110, 10.1111/j.1502-3885.2008.00039.x, 2009.

Andreev, A. A., Schirrmeister, L., Tarasov, P. E., Ganopolski, A., Brovkin, V., Siegert, C., Wetterich, S., and Hubberten, H. W.: Vegetation and climate history in the Laptev Sea region (Arctic Siberia) during Late Quaternary inferred from pollen records, Quaternary Science Reviews, 30, 2182-2199, 10.1016/j.quascirev.2010.12.026, 2011.

Arkhangelov, A., Mikhalev, D., and Nikolaev, V.: Rekonstruktsiya uslovii formirovaniya mnogoletnei merzloty i paleoklimatov Severnoi Evrazii (Reconstruction of formation conditions of permafrost and palaeoclimate of northern Eurasia), in: Razvitie oblasti mnnogoletnei merzloty i periglyatsial'noi zony Severnoi Evrazii i usloviya rasseleniya drevnego cheloveka (History of Permafrost Regions and Periglacial Zones of Northern Eurasia and Conditions of Old Human Settlement), edited by: Velichko, A., Arkhangelov, A., and Borisova, O., RAN Publishing, Moscow, 85-109, 1996.

Blinov, A., Alfimov, V., Beer, J., Gilichinsky, D., Schirrmeister, L., Kholodov, A., Nikolskiy, P., Opel, T., Tikhomirov, D., and Wetterich, S.: Ratio of Cl-36/Cl in ground ice of east Siberia and its application for chronometry, Geochem. Geophys. Geosyst., 10, 12, 10.1029/2009gc002548, 2009.

Boereboom, T., Samyn, D., Meyer, H., and Tison, J. L.: Stable isotope and gas properties of two climatically contrasting (Pleistocene and Holocene) ice wedges from Cape Mamontov Klyk, Laptev Sea, northern Siberia, The Cryosphere, 7, 31-46, 10.5194/tc-7-31-2013, 2013.

Bøtter-Jensen, L., Andersen, C. E., Duller, G. A. T., and Murray, A. S.: Developments in radiation, stimulation and observation facilities in luminescence measurements, Radiat Meas, 37, 535-541, 10.1016/S1350-4487(03)00020-9, 2003.

Bronk Ramsey, C.: Bayesian Analysis of Radiocarbon Dates, Radiocarbon, 51, 337-360, 2009.

Dansgaard, W.: Stable isotopes in precipitation, Tellus, 16, 436-468, 1964.

Dereviagin, A. Y., Chizhov, A., Meyer, H., Opel, T., Schirrmeister, L., and Wetterich, S.: Изотопный состав текстурных льдов побережья моря Лаптевых (Isotopic composition of texture ices, Laptev Sea Coast), Kriosfera Zemlii, 17, 27-34, 2013.

Dewald, A., Heinze, S., Jolie, J., Zilges, A., Dunai, T., Rethemeyer, J., Melles, M., Staubwasser, M., Kuczewski, B., Richter, J., Radtke, U., von Blanckenburg, F., and Klein, M.: CologneAMS, a dedicated center for accelerator mass spectrometry in Germany, Nuclear Instruments & Methods in Physics Research Section B-Beam Interactions with Materials and Atoms, 294, 18-23, 10.1016/j.nimb.2012.04.030, 2013.

Duller, G.: Analyst v4. 31.7 user manual, Aberystwyth Luminescence Research Laboratory, Aberystwyth University, 77 pp, 2015.

Ewing, S. A., Paces, J. B., O'Donnell, J. A., Jorgenson, M. T., Kanevskiy, M. Z., Aiken, G. R., Shur, Y., Harden, J. W., and Striegl, R.: Uranium isotopes and dissolved organic carbon in loess permafrost: Modeling the age of ancient ice, Geochim. Cosmochim. Acta, 152, 143-165, 10.1016/j.gca.2014.11.008, 2015.

French, H., and Shur, Y.: The principles of cryostratigraphy, Earth-Sci. Rev., 101, 190-206, 10.1016/j.earscirev.2010.04.002, 2010.

Fritz, M., Wetterich, S., Schirrmeister, L., Meyer, H., Lantuit, H., Preusser, F., and Pollard, W. H.: Eastern Beringia and beyond: Late Wisconsinan and Holocene landscape dynamics along the Yukon Coastal Plain, Canada, Paleogeogr. Paleoclimatol. Paleoecol., 319, 28-45, 10.1016/j.palaeo.2011.12.015, 2012.

Galbraith, R. F., Roberts, R. G., Laslett, G. M., Yoshida, H., and Olley, J. M.: Optical dating of single and multiple grains of quartz from jinmium rock shelter, northern Australia, part 1, Experimental design and statistical models, Archaeometry, 41, 339-364, DOI 10.1111/j.1475-4754.1999.tb00987.x, 1999.

Ganopolski, A., and Calov, R.: The role of orbital forcing, carbon dioxide and regolith in 100 kyr glacial cycles, Climate of the Past, 7, 1415-1425, 10.5194/cp-7-1415-2011, 2011.

Goslar, T., Czernik, J., and Goslar, E.: Low-energy C-14 AMS in Poznan Radiocarbon Laboratory, Poland, Nucl Instrum Meth B, 223, 5-11, 10.1016/j.nimb.2004.04.005, 2004.

Gravis, G.: Cyclicity of thermokarst at the coastal lowlands during the late Pleistocene and Holocene, Publications of the 3rd International Permafrost Conference, 1978, 283-287,

Grootes, P. M., Nadeau, M. J., and Rieck, A.: C-14-AMS at the Leibniz-Labor: radiometric dating and isotope research, Nuclear Instruments & Methods in Physics Research Section B-Beam Interactions with Materials and Atoms, 223, 55-61, 10.1016/j.nimb.2004.04.015, 2004.

Günther, F., Overduin, P. P., Sandakov, A. V., Grosse, G., and Grigoriev, M. N.: Short- and long-term thermo-erosion of ice-rich permafrost coasts in the Laptev Sea region, Biogeosciences, 10, 4297-4318, 10.5194/bg-10-4297-2013, 2013.

Huntley, D., and Baril, M.: The K content of the K-feldspars being measured in optical dating or in thermoluminescence dating, Ancient TL, 15, 11-13, 1997.

Ivanov, O.: Stratigraphy and correlation of Neogene and Quaternary deposits in subarctic plains of East Yakutia, in: Problemy izucheniya chetvertichnogo perioda (Problems of the Quaternary Period Study), Nauka, Moscow, 202-211, 1972.

Kaplina, T. N., and Lozhkin, A. V.: Age and History of Accumulation of the "Ice Complex" of the Maritime Lowlands of Yakutiya, in: Late Quaternary Environments of the Soviet Union, NED - New edition ed., University of Minnesota Press, 147-152, 1984.

Kienast, F., Wetterich, S., Kuzmina, S., Schirrmeister, L., Andreev, A. A., Tarasov, P., Nazarova, L., Kossler, A., Frolova, L., and Kunitsky, V. V.: Paleontological records indicate the occurrence of open woodlands in a dry inland climate at the present-day Arctic coast in western Beringia during the Last Interglacial, Quaternary Science Reviews, 30, 2134-2159, 10.1016/j.quascirev.2010.11.024, 2011.

Konishchev, V., and Kolesnikov, S.: Osobennosti stroeniya i sostava pozdnekainozoiskikh otlozheniyakh v obnazhenii Oyagosskii Yar (Peculiarities of structure and composition of late Cenozoic deposits in the section of Oyogossky Yar). Problemy Kriolitologii (Problems of Cryolithology), IX, 107-117, 1981.

Krbetschek, M. R., Gotze, J., Dietrich, A., and Trautmann, T.: Spectral information from minerals relevant for luminescence dating, Radiat Meas, 27, 695-748, Doi 10.1016/S1350-4487(97)00223-0, 1997.

Kreutzer, S., Schmidt, C., Fuchs, M. C., Dietze, M., Fischer, M., and Fuchs, M.: Introducing an R package for luminescence dating analysis, Ancient TL, 30, 1-8, 2012.

Kulig, G.: Erstellung einer Auswertesoftware zur Altersbestimmung mittels Lumineszenzverfahren unter spezieller Beruecksichtigung radioaktiver Ungleichgewichte in der 238-U-Zerfallsreihe, BSc, Faculty of Mathematics and Network Computing, TU Bergakademie Freiberg, Freiberg, 2005.

Kunitsky, V.: Khimicheskii sostav ledinykh zhil ledovogo kompleksa (Chemical composition of continuous grown ice-wedges of the Ice Complex), in: Cryolithozone and Groundwater of Siberia, Part I: Morphology of the Cryolithozone, edited by: Klimovski, I., Shepelev, V., and Lyubomirov, A., Melnikov Permafrost Institute Publishing, Yakutsk, 93-117, 1996.

Lachenbruch, A. H.: Mechanics of Thermal Contraction Cracks and Ice-Wedge Polygons in Permafrost, Geological Society of America Special Papers, 70, 1-66, 10.1130/SPE70-p1, 1962.

Lachniet, M. S., Lawson, D. E., and Sloat, A. R.: Revised C-14 dating of ice wedge growth in interior Alaska (USA) to MIS 2 reveals cold paleoclimate and carbon recycling in ancient permafrost terrain, Quat. Res., 78, 217-225, 10.1016/j.yqres.2012.05.007, 2012.

Laskar, J., Robutel, P., Joutel, F., Gastineau, M., Correia, A. C. M., and Levrard, B.: A long-term numerical solution for the insolation quantities of the Earth, Astronomy & Astrophysics, 428, 261-285, 10.1051/0004-6361:20041335, 2004.

Leffingwell, E. D. K.: Ground-ice wedges - The dominant form of ground ice on the north coast of Alaska, J Geol, 23, 635-654, 1915.

Mackay, J. R.: Oxygen isotope variations in permafrost, Tuktoyaktuk Peninsula area, Northwest Territories, Current Research, Part B, Geological Survey of Canada, Paper 83-1B, 67-74, 1983.

Merlivat, L., and Jouzel, J.: Global Climatic Interpretation of the Deuterium-Oxygen 18 Relationship for Precipitation, Journal of Geophysical Research-Oceans and Atmospheres, 84, 5029-5033, 10.1029/JC084iC08p05029, 1979.

Meyer, H., Schönicke, L., Wand, U., Hubberten, H. W., and Friedrichsen, H.: Isotope studies of hydrogen and oxygen in ground ice - Experiences with the equilibration technique, Isot. Environ. Health Stud., 36, 133-149, 10.1080/10256010008032939, 2000.

Meyer, H., Dereviagin, A. Y., Siegert, C., and Hubberten, H.-W.: Paleoclimate studies on Bykovsky Peninsula, North Siberia-hydrogen and oxygen isotopes in ground ice, Polarforschung, 70, 37-51, 2002a.

Meyer, H., Dereviagin, A. Y., Siegert, C., Schirrmeister, L., and Hubberten, H. W.: Palaeoclimate reconstruction on Big Lyakhovsky Island, North Siberia - Hydrogen and oxygen isotopes in ice wedges, Permafrost Periglacial Process., 13, 91-105, 10.1002/ppp.416, 2002b.

Meyer, H., Schirrmeister, L., Andreev, A., Wagner, D., Hubberten, H. W., Yoshikawa, K., Bobrov, A., Wetterich, S., Opel, T., Kandiano, E., and Brown, J.: Lateglacial and Holocene isotopic and environmental history of northern coastal Alaska - Results from a buried ice-wedge system at Barrow, Quaternary Science Reviews, 29, 3720-3735, 10.1016/j.quascirev.2010.08.005, 2010a.

Meyer, H., Schirrmeister, L., Yoshikawa, K., Opel, T., Wetterich, S., Hubberten, H. W., and Brown, J.: Permafrost evidence for severe winter cooling during the Younger Dryas in northern Alaska, Geophys. Res. Lett., 37, L03501, 10.1029/2009gl041013, 2010b.

Meyer, H., Opel, T., Laepple, T., Dereviagin, A. Y., Hoffmann, K., and Werner, M.: Long-term winter warming trend in the Siberian Arctic during the mid-to late Holocene, Nat. Geosci., 8, 122-125, 10.1038/ngeo2349, 2015.

Michel, F. A.: Isotope investigations of permafrost waters in northern Canada, Department of Earth Sciences, University of Waterloo, 1982.

Murray, A. S., and Wintle, A. G.: Luminescence dating of quartz using an improved single-aliquot regenerative-dose protocol, Radiat Meas, 32, 57-73, Doi 10.1016/S1350-4487(99)00253-X, 2000.

Murray, A. S., and Wintle, A. G.: The single aliquot regenerative dose protocol: potential for improvements in reliability, Radiat Meas, 37, 377-381, 10.1016/S1350-4487(03)00053-2, 2003.

Nagaoka, D., Saijo, K., and Fukuda, M.: Sedimental environment of the Edoma in high Arctic eastern Siberia, Proceedings of the Third Symposium on the joint Siberian permafrost Studies between Japan and Russia in 1994, Tsukuba, Japan, 1995, 8-13, 1995.

North Greenland Ice Core Project members: High-resolution record of Northern Hemisphere climate extending into the last interglacial period, Nature, 431, 147-151, 10.1038/nature02805, 2004.

Opel, T., Dereviagin, A. Y., Meyer, H., Schirrmeister, L., and Wetterich, S.: Palaeoclimatic Information from Stable Water Isotopes of Holocene Ice Wedges on the Dmitrii Laptev Strait, Northeast Siberia, Russia, Permafrost Periglacial Process., 22, 84-100, 10.1002/ppp.667, 2011.

Opel, T., Laepple, T., Meyer, H., Dereviagin, A., and Wetterich, S.: Northeast Siberian ice wedges confirm Arctic winter warming over the past two millennia, Holocene, in revision.

Petoukhov, V., Ganopolski, A., Brovkin, V., Claussen, M., Eliseev, A., Kubatzki, C., and Rahmstorf, S.: CLIMBER-2: a climate system model of intermediate complexity. Part I: model description and performance for present climate, Clim. Dyn., 16, 1-17, Doi 10.1007/Pl00007919, 2000.

Porter, T. J., Froese, D. G., Feakins, S. J., Bindeman, I. N., Mahony, M. E., Pautler, B. G., Reichart, G. J., Sanborn, P. T., Simpson, M. J., and Weijers, J. W. H.: Multiple water isotope proxy reconstruction of extremely low last glacial

temperatures in Eastern Beringia (Western Arctic), Quaternary Science Reviews, 137, 113-125, 10.1016/j.quascirev.2016.02.006, 2016.

Reimer, P. J., Bard, E., Bayliss, A., Beck, J. W., Blackwell, P. G., Bronk Ramsey, C., Buck, C. E., Cheng, H., Edwards, R. L., Friedrich, M., Grootes, P. M., Guilderson, T. P., Haflidason, H., Hajdas, I., Hatte, C., Heaton, T. J., Hoffmann, D. L.,

5   Hogg, A. G., Hughen, K. A., Kaiser, K. F., Kromer, B., Manning, S. W., Niu, M., Reimer, R. W., Richards, D. A., Scott, E. M., Southon, J. R., Staff, R. A., Turney, C. S. M., and van der Plicht, J.: IntCal13 and Marine13 Radiocarbon Age Calibration Curves 0–50,000 Years cal BP, Radiocarbon, 55, 1869-1887, 2013.

Rethemeyer, J., Fulop, R. H., Hofle, S., Wacker, L., Heinze, S., Hajdas, I., Patt, U., Konig, S., Stapper, B., and Dewald, A.: Status report on sample preparation facilities for C-14 analysis at the new CologneAMS center, Nuclear Instruments &

10   Methods in Physics Research Section B-Beam Interactions with Materials and Atoms, 294, 168-172, 10.1016/j.nimb.2012.02.012, 2013.

Rudaya, N., Protopopov, A., Trofimova, S., Plotnikov, V., and Zhilich, S.: Landscapes of the 'Yuka' mammoth habitat: A palaeobotanical approach, Rev. Palaeobot. Palynology, 214, 1-8, 10.1016/j.revpalbo.2014.12.003, 2015.

Schirrmeister, L., Oezen, D., and Geyh, M. A.: Th-230/U dating of frozen peat, Bol'shoy Lyakhovsky Island (Northern

15   Siberia), Quat. Res., 57, 253-258, 10.1006/qres.2001.2306, 2002.

Schirrmeister, L., Grosse, G., Kunitsky, V., Meyer, H., Derivyagin, A., and Kuznetsova, T.: Permafrost, periglacial and paleo-environmental studies on New Siberian Islands, in: Russian-German Cooperation System Laptev Sea The Expeditions Lena 2002, edited by: Grigoriev, M., Rachold, V., Bolshiyanov, D., Pfeiffer, E., Schirrmeister, L., Wagner, D., and Hubberten, H., Reports on Polar and Marine Research, Alfred Wegener Institute for Polar and Marine Research

20   Bremerhaven, 195–314, 2003a.

Schirrmeister, L., Grosse, G., Schwamborn, G., Andreev, A. A., Meyer, H., Kunitsky, V. V., Kuznetsova, T. V., Dorozhkina, M. V., Pavlova, E. Y., Bobrov, A. A., and Oezen, D.: Late Quaternary History of the Accumulation Plain North of the Chekanovsky Ridge (Lena Delta, Russia): A Multidisciplinary Approach, Polar Geography, 27, 277-319, 10.1080/789610225, 2003b.

25   Schirrmeister, L., Wetterich, S., Kunitsky, V., Tumskoy, V., Dobrynin, D., Derevyagyn, A., Opel, T., Kienast, F., Kuznetsova, T., and Gorodinsky, A.: Palaeoenviromental studies on the Oyogos Yar coast, in: The Expedition LENA - NEW SIBERIAN ISLANDS 2007 during the International Polar Year (IPY) 2007/2008, edited by: Boike, J., Bol'shiyanov, D., Schirrmeister, L., and Wetterich, S., Reports on Polar and Marine Research, Alfred Wegener Institute for Polar and Marine Research Bremerhaven, 85-154, 2008.

30   Schirrmeister, L., Grosse, G., Schnelle, M., Fuchs, M., Krbetschek, M., Ulrich, M., Kunitsky, V., Grigoriev, M., Andreev, A., Kienast, F., Meyer, H., Babiy, O., Klimova, I., Bobrov, A., Wetterich, S., and Schwamborn, G.: Late Quaternary paleoenvironmental records from the western Lena Delta, Arctic Siberia, Paleogeogr. Paleoclimatol. Paleoecol., 299, 175-196, 10.1016/j.palaeo.2010.10.045, 2011a.

Schirrmeister, L., Kunitsky, V., Grosse, G., Wetterich, S., Meyer, H., Schwamborn, G., Babiy, O., Derevyagin, A., and

35   Siegert, C.: Sedimentary characteristics and origin of the Late Pleistocene Ice Complex on north-east Siberian Arctic coastal lowlands and islands - A review, Quat. Int., 241, 3-25, 10.1016/j.quaint.2010.04.004, 2011b.

Schirrmeister, L., Froese, D., Tumskoy, V., Grosse, G., and Wetterich, S.: Yedoma: Late Pleistocene Ice-Rich Syngenetic Permafrost of Beringia, in: Encyclopedia of Quaternary Science (Second Edition), edited by: Elias, S. A., Elsevier, Amsterdam, 542-552, 2013.

40   Schirrmeister, L., Meyer, H., Andreev, A., Wetterich, S., Kienast, F., Bobrov, A., Fuchs, M., Sierralta, M., and Herzschuh, U.: Late Quaternary paleoenvironmental records from the Chatanika River valley near Fairbanks (Alaska), Quaternary Science Reviews, 147, 259-278, 10.1016/j.quascirev.2016.02.009, 2016.

Schwamborn, G., Meyer, H., Fedorov, G., Schirrmeister, L., and Hubberten, H. W.: Ground ice and slope sediments archiving late Quaternary paleoenvironment and paleoclimate signals at the margins of El'gygytgyn Impact Crater, NE

45   Siberia, Quat. Res., 66, 259-272, 10.1016/j.yqres.2006.06.007, 2006.

Streletskaya, I. D., Vasiliev, A. A., Oblogov, G. E., and Tokarev, I. V.: Reconstruction of paleoclimate of Russian Arctic in the Late Pleistocene–Holocene on the basis of isotope study of ice wedges, Kriosfera Zemli, 19, 86-94, 2015.

Stuiver, M., and Polach, H. A.: Reporting of 14C Data - Discussion, Radiocarbon, 19, 355-363, 1977.

Tomirdiaro, S. V.: Periglacial Landscapes and Loess Accumulation in the Late Pleistocene Arctic and Subarctic, in: Late

50   Quaternary Environments of the Soviet Union, NED - New edition ed., University of Minnesota Press, 141-146, 1984.

Tumskoy, V.: Osobennosti kriolitogeneza otlozhenii severnoi Yakutii v srednem Neopleistotsene-Golotsene (Peculiarities of cryolithogenesis in northern Yakutia from the Middle Neopleistocene to the Holocene), Kriosfera Zemli, 16, 12-21, 2012.

Vaikmäe, R.: Oxygen isotopes in permafrost and ground ice: A new tool for paleoclimatic investigations, 5th Working Meeting Isotopes in Nature, Leipzig, September 1989, Proceedings, 1989, 543-553,

5   Van Everdingen, R. e.: Multi-language glossary of permafrost and related ground-ice terms (revised 2005), National Snow and Ice Data Center/World Data Center for Glaciology, Boulder, 1998.

Vasil'chuk, Y., and Vasil'chuk, A.: Spatial distribution of mean winter air temperatures in Siberian permafrost at 20-18ka BP using oxygen isotope data, Boreas, 43, 678-687, 10.1111/bor.12033, 2014.

Vasil'chuk, Y. K., van der Plicht, J., Jungner, H., Sonninen, E., and Vasil'chuk, A. C.: First direct dating of Late Pleistocene
10   ice-wedges by AMS, Earth Planet. Sci. Lett., 179, 237-242, 10.1016/S0012-821X(00)00122-9, 2000.

Vasil'chuk, Y. K., Vasil'chuk, A. C., Rank, D., Kutschera, W., and Kim, J. C.: Radiocarbon dating of δ18O-δD plots in Late Pleistocene ice-wedges of the Duvanny Yar (Lower Kolynia River, Northern Yakutia), Radiocarbon, 43, 541-553, 2001.

Vasil'chuk, Y. K.: Syngenetic Ice Wedges: Cyclical Formation, Radiocarbon Age and Stable Isotope Records by Yurij K. Vasil'chuk, Moscow University Press, Moscow, 2006. 404pp. ISBN 5-211-05212-9, Permafrost Periglacial Process., 24, 82-
15   93, 10.1002/ppp.1764, 2013.

Walter, K. M., Edwards, M. E., Grosse, G., Zimov, S. A., and Chapin, F. S.: Thermokarst lakes as a source of atmospheric CH4 during the last deglaciation, Science, 318, 633-636, 10.1126/science.1142924, 2007.

Wetterich, S., Kuzmina, S., Andreev, A. A., Kienast, F., Meyer, H., Schirrmeister, L., Kuznetsova, T., and Sierralta, M.: Palaeoenvironmental dynamics inferred from late Quaternary permafrost deposits on Kurungnakh Island, Lena Delta,
20   Northeast Siberia, Russia, Quaternary Science Reviews, 27, 1523-1540, 10.1016/j.quascirev.2008.04.007, 2008.

Wetterich, S., Schirrmeister, L., Andreev, A. A., Pudenz, M., Plessen, B., Meyer, H., and Kunitsky, V. V.: Eemian and Late Glacial/Holocene palaeoenvironmental records from permafrost sequences at the Dmitry Laptev Strait (NE Siberia, Russia), Paleogeogr. Paleoclimatol. Paleoecol., 279, 73-95, 10.1016/j.palaeo.2009.05.002, 2009.

Wetterich, S., Rudaya, N., Tumskoy, V., Andreev, A. A., Opel, T., Schirrmeister, L., and Meyer, H.: Last Glacial Maximum
25   records in permafrost of the East Siberian Arctic, Quaternary Science Reviews, 30, 3139-3151, 10.1016/j.quascirev.2011.07.020, 2011.

Wetterich, S., Tumskoy, V., Rudaya, N., Andreev, A. A., Opel, T., Meyer, H., Schirrmeister, L., and Huls, M.: Ice Complex formation in arctic East Siberia during the MIS3 Interstadial, Quaternary Science Reviews, 84, 39-55, 10.1016/j.quascirev.2013.11.009, 2014.

30   Wetterich, S., Tumskoy, V., Rudaya, N., Kuznetsov, V., Maksimov, F., Opel, T., Meyer, H., Andreev, A. A., and Schirrmeister, L.: Ice Complex permafrost of MIS5 age in the Dmitry Laptev Strait coastal region (East Siberian Arctic), Quaternary Science Reviews, 147, 298-311, 10.1016/j.quascirev.2015.11.016, 2016.

Wolff, E. W., Chappellaz, J., Blunier, T., Rasmussen, S. O., and Svensson, A.: Millennial-scale variability during the last glacial: The ice core record, Quaternary Science Reviews, 29, 2828-2838, 10.1016/j.quascirev.2009.10.013, 2010.

Table 1. Synopsis of the stratigraphic units exposed on the Dmitry Laptev Strait according to the latest compilation by Tumskoy (2012) and updates from this study. Grey shaded strata were not found at the Oyogos Yar coast (OY), but are described from Bol'shoy Lyakhovsky Island (BL). MIS refers to Marine Isotope Stage and SIW to syngenetic ice wedges. Radiocarbon ages are given as mean calibrated ages b2k. Further information is given in the following studies from both sides of the Dmitry Laptev Strait:

(a) this study, (b) (Schirrmeister et al., 2011b), (c) (Andreev et al., 2009), (d) (Wetterich et al., 2009), (e) (Opel et al., 2011) (f) (Wetterich et al., 2011), (g) (Wetterich et al., 2014), (h) (Andreev et al., 2004), (i) (Wetterich et al., 2016), (j) (Schirrmeister et al., 2002)

Stratigraphic unit [a]	Local stratigraphy	Period	Description	BL age (kyr b2k)	OY age (kyr b2k)	Dating method	MIS	SIW presence	Reference
VIII	Cover deposits	Holocene	Holocene cover on top of Yedoma IC	10.9 to 0	11.0 to 0	^{14}C-AMS	1	Yes	a, b, c
VII	Alas (Laptev Suite)	Holocene	Thermokarst palustrine deposits	8.4 to 0	13.0 to 0	^{14}C-AMS	1	Yes	a, b, c, d, e
VI	Alas (Laptev Suite)	Late Glacial to Holocene	Thermokarst lacustrine deposits	14.7 to 8.0	18.1 to 12.7	^{14}C-AMS	2-1	No	a, b, c, d
--	Sartan (Yana Suite)	Stadial (LGM	Yedoma IC deposits	30.0 to 26.7	--	^{14}C-AMS	2	Yes	f
V	Molotkov (Oyogos Suite)	Interstadial	Taberal Yedoma IC deposits	>54 to 37.3	46.0 to 40.1	^{14}C-AMS	3	No	a, b, c, d
IV	Molotkov (Oyogos Suite)	Interstadial	Yedoma IC deposits	>59 to 32.5	49.4 to 36.3	^{14}C-AMS	3	Yes	a, b, c, g
--	Zyryanian (unit IV in Andreev et al. (2004))	Stadial	Floodplain deposits	57±10, 68±14, 77±12, 77±14	--	IRSL	4	Yes	h
III	Kazantsevo (Krest Yuryakh Suite)	Interstadial	Thermokarst lacustrine and palustrine deposits	--	102.4±9.7	IRSL	5	No	a, d,hi
II	Kazantsevo (Bychchagy Suite)	Stadial	Buchchagy IC deposits	89±5, 93±5, 117+19/-14, 126+16/-13	--	[230]Th/U	5	Yes	a, i
I	Keremesitsko (Kuchchugui Suite)	Stadial	Floodplain deposits	99±15 102±16	112.5±9.6	IRSL	5	Yes	a, h
--	Keremesitsko (Zimov'e layer)	Stadial	Palaeo active layer	134±22	--	IRSL	6-5	No	h
--	Keremesitsko (Yukagir Suite)	Interstadial	Yukagir IC deposits	200.9±3.4	--	[230]Th/U	7	Yes	j

Table 2. IRSL samples Oy7-07-01 (unit I) and Oy7-08-25 (unit III) with all paleodose and dose rate parameters used for final age calculation (n = number of aliquots, CAM = Central Age Model according to (Galbraith et al., 1999) m asl = meter above sea level, m bs = meter below surface).

ID		Oy7-07-01	Oy7-08-25
Paleodose parameters:			
n		49	5
mean	(Gy)	288.4 ± 4.0	270.8 ± 8.0
Standard deviation	(%)	9.6	6.6
skewness		0.4	0.2
Coefficient of variation	(%)	6.7	6.3
CAM	(Gy)	286.9 ± 3.9	-
Dose rate parameters:			
^{238}U	(Bq kg^{-1})	24.77 ± 2.55	33.43 ± 0.88
^{232}Th	(Bq kg^{-1})	31.75 ± 1.12	38.14 ± 1.88
^{40}K	(Bq kg^{-1})	572.95 ± 7.99	528.11 ± 3.05
Water content	(%)	30.5	27.5
Height / cover thickness	(m asl / m bs)	1.5 / 24	4 / 22
Total dose rate	(Gy kyr^{-1})	2.6	2.6
Age	**(kyr)**	**112.5 ± 9.6**	**102.4 ± 9.7**

Table 3. Radiocarbon ages and calibrated ages (95.4% probability) of sediment samples from Oyogos Yar coast. NaN indicates that the calibration failed and no calibrated age is available.

Sample ID	Unit	Height (m asl)	Lab ID	Conventional age (yr BP)	Calibrated age (mean) (yr b2k)	Remarks
Field campaign 2002 (this study)						
Oya-2-1	VIII	0.4 m bs	KIA 25724	7985±40	9052-8708 (8880)	
Oya-2-5	VIII	1.9 m bs	KIA 25725	8345±40	9521-9321 (9421)	
Oya-2-8	VIII	3.0 m bs	KIA 25726	9645±35	11,237-10,842 (11,040)	
Oya-4-1	IV	17	KIA 25731	>36,690	> 40,921 (-)	
Oya-6-1	I	2.5	KIA 25732	>43,350	> 44,506 (-)	leached residue
				41,520+1030/-910	47,139-43,297 (45,218)	humic acid
Oya-3-11	III	2	KIA 25730	47,700+1380/-1180	50,906-45,666 (48,286)	IW cast below unit IV
Field campaign 2007 – Sequence A: Buchchagy Ice Complex (Wetterich et al., 2016)						
Oy7-10-09	II	6.2	Poz-51638	>49,000	-	Upper peat
Oy7-10-04	II	3.3	Poz-51637	>51,000	-	Lower peat
Field campaign 2007 – Sequence B: Yedoma Ice Complex (Schirrmeister et al., 2011b)						
Oy7-08-63	IV	27.0	KIA37638	32,220+370/-350	37,199-35,324 (36,262)	
Oy7-08-62	IV	26.5	KIA37637	34,630+420/-400	40,208-38,435 (39,322)	
Oy7-08-57	IV	24.0	KIA37636	38,600+930/-830	44,365-41,551 (42,958)	
Oy7-08-53	IV	22.0	KIA37635	44,900+1230/-1060	NaN-46,593 (NaN)	
Oy7-08-47	IV	19.2	KIA37634	40,850+1750/-1440	48,313-42,357 (45,335)	
Oy7-08-42	IV	17.1	KIA37633	48,540+1750/-1440	53,128-45,594 (49,361)	
Oy7-08-38	IV	15.5	KIA37632	44,840+1270/-1100	NaN-46,238 (NaN)	
Oy7-08-37	IV	12.0	KIA37631	43,860+1270/-1090	49,686-45,380 (47,533)	
Oy7-08-32	IV	9.5	KIA37630	41,420+1040/-920	46,909-43,225 (45,067)	
Field campaign 2007 – Sequence C: Taberal Yedoma Ice Complex to Holocene (Wetterich et al., 2009))						
Oy7-11-14	VII	11.1	KIA35234	3325±35	3690-3513 (3602)	
Oy7-11-12	VII	10.1	KIA35233	8335±45	9524-9198 (9361)	
Oy7-11-10	VII	8.8	KIA35232	8260±40	9461-9144 (9303)	
Oy7-11-09	VII	8.6	KIA36687	9985±35	11,665-11,322 (11,494)	
Oy7-11-08	VII	8.3	KIA36686	11,145±40	13,155-12,942 (13,049)	
Oy7-11-07	VI	8.0	KIA35231	14,830+70/-60	18,299-17,899 (18,099)	
Oy7-11-06	VI	7.7	KIA36688	10,720+40/-35	12,781-12,651 (12,716)	
Oy7-11-04	VI	7.1	KIA35230	11,995±50	14,062-13,786 (13,924)	
Oy7-11-03	V	6.8	KIA35229	41,290+2370/-1830	49,458-42,469 (45,964)	
Oy7-11-01	V	6.0	KIA35228	36,580+1090/-960	40,863-39,333 (40,098)	

Table 4. Radiocarbon ages and calibrated ages (95.4% probability, if not otherwise indicated) of organic remains in Holocene ice-wedge samples of Unit VII

Sample ID	Lab ID	Conventional age (yr BP)	Calibrated age (mean) (yr b2k)	Remarks
Ice wedge Oy7-04 IW2 (Oy7-04-…) (Opel et al., 2011; Opel et al., in revision)				
205	COL3997.1.1	1607 ±49	1659-1438 (1549)	
242	KIA 35630	523 ± 43	690-551 (621)	
247	KIA 35631	3518 ± 31	3927-3751 (3839)	Reworked
263	KIA 35632	412 ± 30	570-380 (475)	
267	KIA 35633	258 ± 51	519-193 (356)	(89.7% probability)
274	KIA 35634	488 ± 58	696-382 (539)	
290	KIA 35635	1479 ± 106	1659-1232 (1446)	
Ice wedge Oy7-11 IW2 (Oy7-11-…) (Opel et al., 2011)				
138	KIA 35636	8959 ± 43	10,278-9970 (10,124)	Redistributed
162	KIA 35637	8300 ± 43	9486-9188 (9337)	Redistributed
189	KIA 35638	857 ± 43	956-737 (847)	
Ice wedge Oy7-11 IW7 (Oy7-11-…) (Opel et al., in revision)				
719	KIA 40385	1858 ± 60	1976-1674 (1825)	
723	KIA 40386	1868 ± 36	1931-1765 (1848)	
740	KIA 40387	1081 ± 22	1104-984 (1044)	
747	KIA 40388	1098 ± 24	1100-1005 (1053)	
796	KIA 40390	$F^{14}C$ 1.2661 ± 0.005	20-18(19)	Post-bomb
820	KIA 40391	225 ± 25	358-198 (278)	(84.5% probability)
Hy27	COL1925.1.1	1579 ± 43	1606-1429 (1518)	
Hy31	KIA 40393	14,200 ± 71	17,575-17,108 (17,342)	Redistributed
Hy40	KIA 40394	6640 ± 50	7637-7487 (7562)	Redistributed

Table 5. Stable isotope (δ¹⁸O, δD and *d* excess) minimum, mean and maximum values, standard deviations as well as slopes and intercept in the δ¹⁸O-δD diagram for all considered ice wedges. Ice wedges marked with an asterisk contain samples attributed to Unit IV and Unit VIII, respectively.

Ice wedge (profiles/group of samples)	Altitude (m a.s.l.)	Width (m)	Samples (n)	$\delta^{18}O$ min (‰)	$\delta^{18}O$ mean (‰)	$\delta^{18}O$ max (‰)	$\delta^{18}O$ sd (‰)	δD min (‰)	δD mean (‰)	δD max (‰)	δD sd (‰)	d min (‰)	d mean (‰)	d max (‰)	d sd (‰)	Slope	Intercept	R^2
Unit VIII Holocene cover deposits																		
Oy7-08 IW5	36.0	0.5	2	-26.55	-25.71	-24.87	1.18	-201.1	-195.6	-190.1	7.8	8.9	10.1	11.3	1.7	6.57	-26.58	1.00
Oy7-08 IW4	35.0	10.2	26	-27.81	-25.86	-20.89	1.44	-216.9	-200.2	-158.8	12.3	2.6	6.7	9.0	1.5	8.47	18.81	0.99
Oy7-08 IW3*	30.0	5.0	11	-27.94	-26.43	-24.38	1.14	-216.8	-203.7	-183.9	10.2	5.9	7.7	11.1	1.7	9.22	40.26	0.99
Oy7-06 IW2*	20.0	2	8	-27.14	-26.69	-25.84	0.47	-209.3	-205.1	-197.1	4.1	7.6	8.4	9.6	0.7	8.60	24.51	0.98
Texture ice	Several	n/a	3	-20.65	-19.60	-17.59	1.74	-157.1	-148.7	-134.2	12.7	6.6	8.1	10.4	2.0	7.23	-7.02	0.99
Unit VII Holocene palustrine deposits																		
Modern ice veins	11	< 0.08	14	-24.38	-20.74	-18.24	1.61	-186.4	-158.3	-137.3	12.6	4.7	7.7	9.1	1.1	7.79	3.23	0.99
Recent IW parts	11	varying	24	-25.27	-22.68	-18.27	1.66	-193.5	-173.9	-137.5	13.4	4.8	7.6	9.5	1.1	8.03	8.33	0.99
Oy7-04 IW2	10.0	3.2	104	-27.09	-25.10	-21.59	1.26	-207.8	-192.0	-164.2	9.6	6.2	8.8	11.3	1.1	7.58	-1.83	0.99
Oy7-11 IW1	10.0	3.5	119	-26.64	-25.01	-21.62	1.03	-203.9	-192.1	-167.2	7.8	5.1	8.0	9.8	0.9	7.59	-2.19	0.99
Oy7-11 IW7	10.0	2.5	236	-26.53	-24.99	-20.73	0.90	-203.2	-192.4	-159.9	6.9	4.1	7.5	9.3	0.9	7.67	-0.75	0.99
Oy7-02 IW1	8.0	~1.5	14	-26.28	-25.36	-23.41	0.79	-201.3	-194.6	-179.5	6.0	6.5	8.2	9.2	0.9	7.53	-3.76	0.99
Texture ice	Several	n/a	23	-21.93	-17.61	-16.00	1.63	-171.4	-139.7	-124.2	13.2	-3.7	1.2	10.7	4.6	7.57	-6.35	0.88
Unit IV Yedoma Ice Complex deposits																		
Oya-IW3	Ca. 35.0	n/a	8	-32.51	-31.47	-28.27	1.60	-256.0	-246.8	-219.9	13.6	4.0	5.0	6.3	0.9	8.49	20.31	1.00
Oya-IW4	Ca. 35.0	n/a	6	-31.72	-31.41	-31.00	0.26	-249.4	-247.6	-243.5	2.1	2.2	3.7	4.5	0.8	7.55	-10.53	0.84
Oy7-08 IW3*	30.0	5.0	22	-31.68	-29.96	-28.01	1.13	-250.8	-234.8	-218.4	9.5	2.7	4.8	7.2	1.2	8.32	14.41	0.99
Oy7-08 IW1	25.0	5.7	34	-32.72	-31.48	-30.11	0.57	-255.1	-246.7	-236.7	4.1	3.1	5.2	7.1	1.0	7.07	-23.91	0.95
Oy7-06 IW2*	20.0	2.0	14	-30.49	-29.45	-28.05	0.80	-239.6	-228.6	-214.2	7.6	4.3	7.0	10.2	2.0	9.29	44.81	0.95
Oya-IW5	16.0	3.0	15	-33.29	-32.84	-31.90	0.41	-262.1	-258.3	-249.6	3.5	3.8	4.5	5.6	0.6	8.55	22.66	0.98
Oy7-06 IW1	9.0	3.5	34	-31.30	-30.13	-28.01	0.87	-241.8	-233.9	-218.2	6.1	5.2	7.2	9.0	1.0	7.01	-22.69	0.99
Oya-IW2	6.6-7.0	1.5	8	-31.32	-30.96	-30.45	0.36	-241.9	-239.5	-236.3	2.2	7.0	8.1	9.3	0.9	5.95	-55.37	0.94
Oya-IW6	5.0	1.5	6	-33.04	-31.65	-30.39	1.08	-256.0	-246.1	-236.8	7.9	4.7	7.1	8.3	1.4	7.26	-16.31	0.98
Oy7-01 IW4	1.5	0.5	3	-29.71	-29.23	-28.31	0.80	-231.7	-227.6	-220.2	6.4	6.0	6.3	6.5	0.3	8.00	6.45	1.00
Texture ice	Several	n/a	44	-34.45	-26.14	-18.48	4.84	-253.9	-206.2	-150.5	32.0	-10.9	2.9	21.7	9.0	6.51	-36.00	0.97
Unit II Buchchagy Ice Complex deposits																		
Oy7-07 IW1	4.0	1.7	7	-33.52	-33.13	-32.68	0.29	-261.1	-258.3	-255.1	2.1	6.1	6.7	7.2	0.4	6.96	-27.89	0.98
Texture ice	Several	n/a	8	-29.80	-26.71	-23.34	2.55	-233.8	-210.9	-184.9	17.8	-1.9	2.8	9.9	4.0	6.89	-26.83	0.98

Unit I Kuchchugui floodplain deposits																
Oy7-03 IW1+2	3.5	0.4-1.0	5+1	-34.88	-34.11	-32.77	0.75	-273.6	-268.0	-255.1	6.8	1.8	4.9	7.1	1.9	8.74	29.99	0.93
Oy7-03 IW1+5	2.0	0.3-0.4	3+2	-30.15	-29.66	-29.29	0.37	-238.7	-235.0	-231.5	3.3	1.5	2.3	2.8	0.5	8.68	22.46	0.98
Oy7-03 IW4	2.0	0.4	4	-28.35	-28.19	-28.08	0.12	-226.7	-225.6	-224.7	0.9	-0.4	0.0	0.4	0.4	6.70	-36.78	0.82
Oya IW1	1.5	0.75	6	-31.12	-30.67	-30.42	0.26	-243.8	-240.5	-238.6	2.0	4.4	4.8	5.1	0.2	7.41	-13.23	0.99
Texture ice	Several	n/a	10	-29.75	-25.99	-23.09	2.52	-231.8	-210.5	-191.4	15.8	-8.0	-2.6	6.2	4.6	6.24	-48.31	0.99
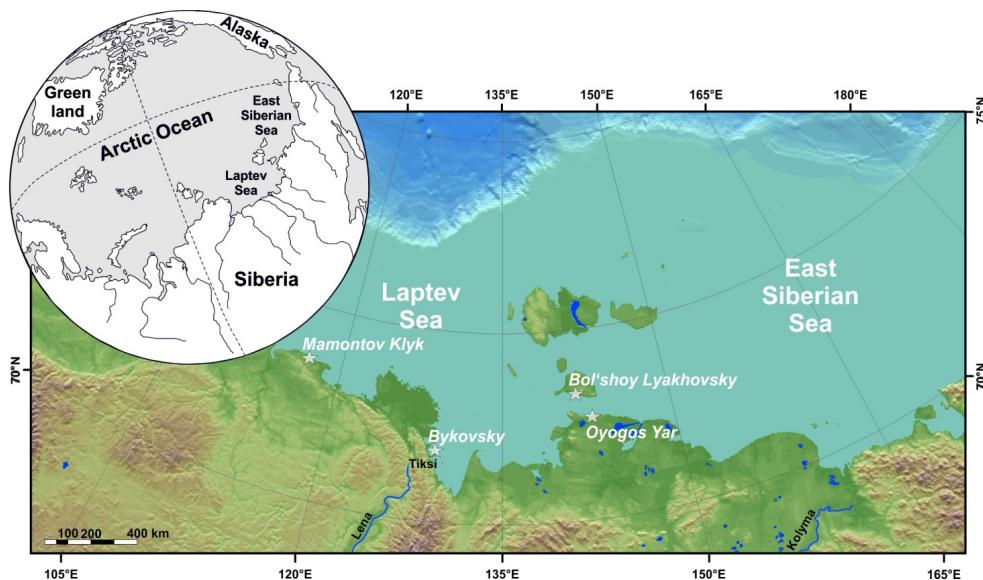
Figure 1. Map of the study region.
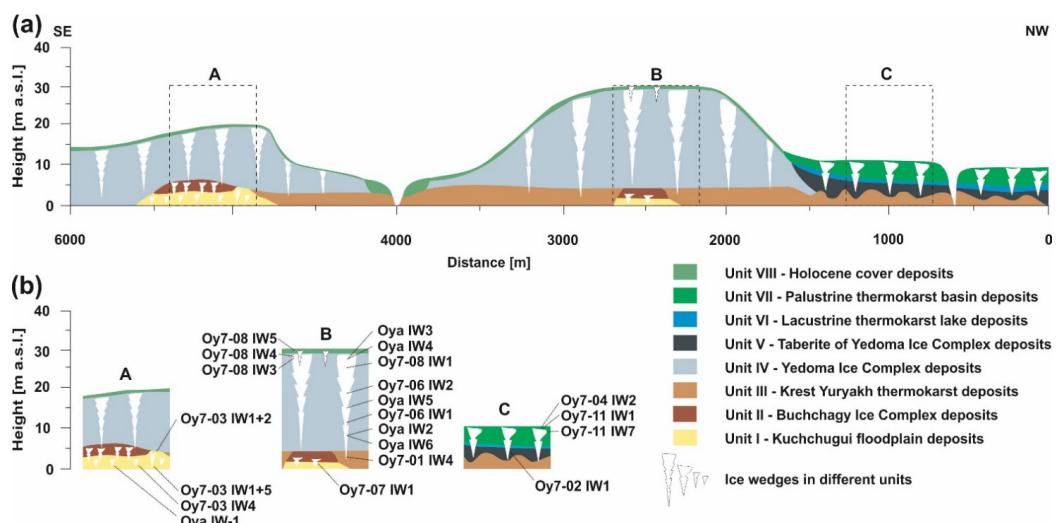
5   **Figure 2. (a) Overall stratigraphic sketch of the Oyogos Yar mainland coast about 30 km west of the Kondrat'eva River mouth indicating the main stratigraphic units, and (b) the approximate positions of the studied ice wedges in three outbreak schemes (sequences A to C). Updated and redrawn after (Blinov et al., 2009).**

Figure 3. Photographs of selected outcrops and ice wedges of different units. CSIW means composite sand-ice wedge.
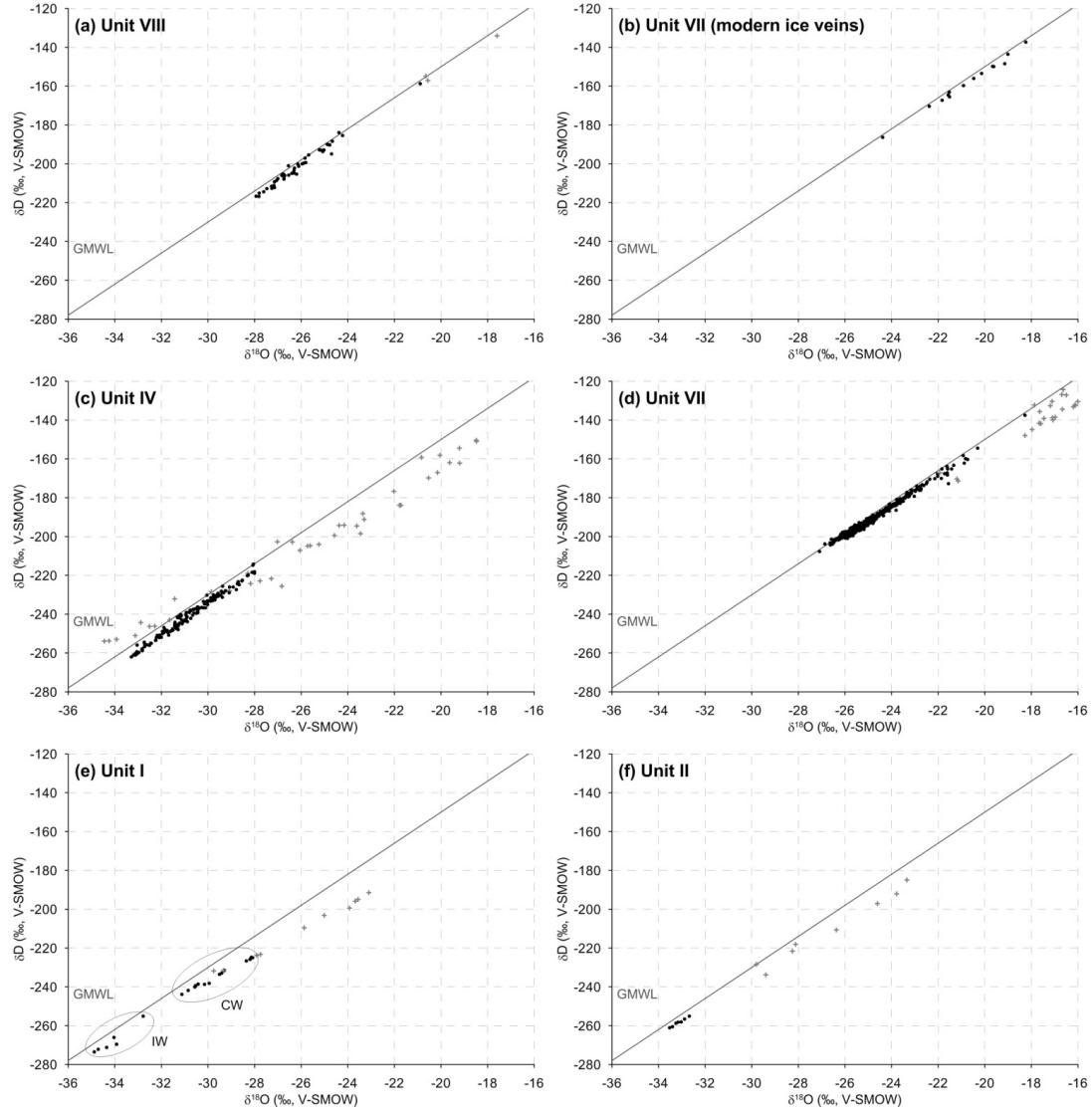
Figure 4. δ¹⁸O-δD diagrams for ice-wedge and texture-ice data attributed to the studied units. Black dots refer to ice-wedge data and grey crosses to texture-ice data. In panel (e) IW indicates ice-wedge samples and CW composite-wedge samples.
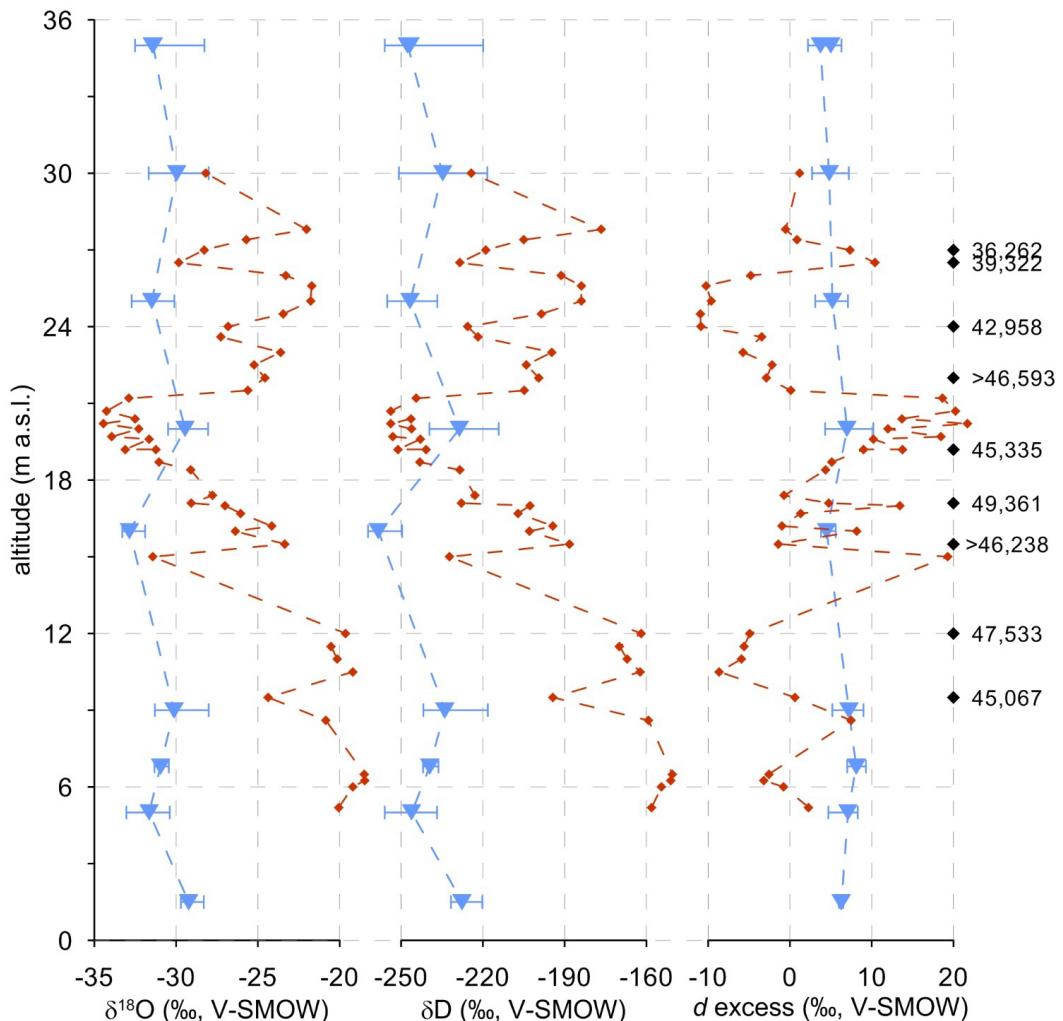
Figure 5. Single δ¹⁸O, δD and *d* excess data of texture ice (red dots) and δ¹⁸O, δD and *d* excess data (min, mean, max) of horizontal ice wedges profiles (blue triangles) of the Yedoma Ice Complex (unit IV) plotted against altitude. Additionally given are radiocarbon ages (mean calibrated yr b2k, in two cases minimum ages) obtained from sediment samples. These ages do not necessarily reflect the age of the ice wedges which are assumed to be younger.
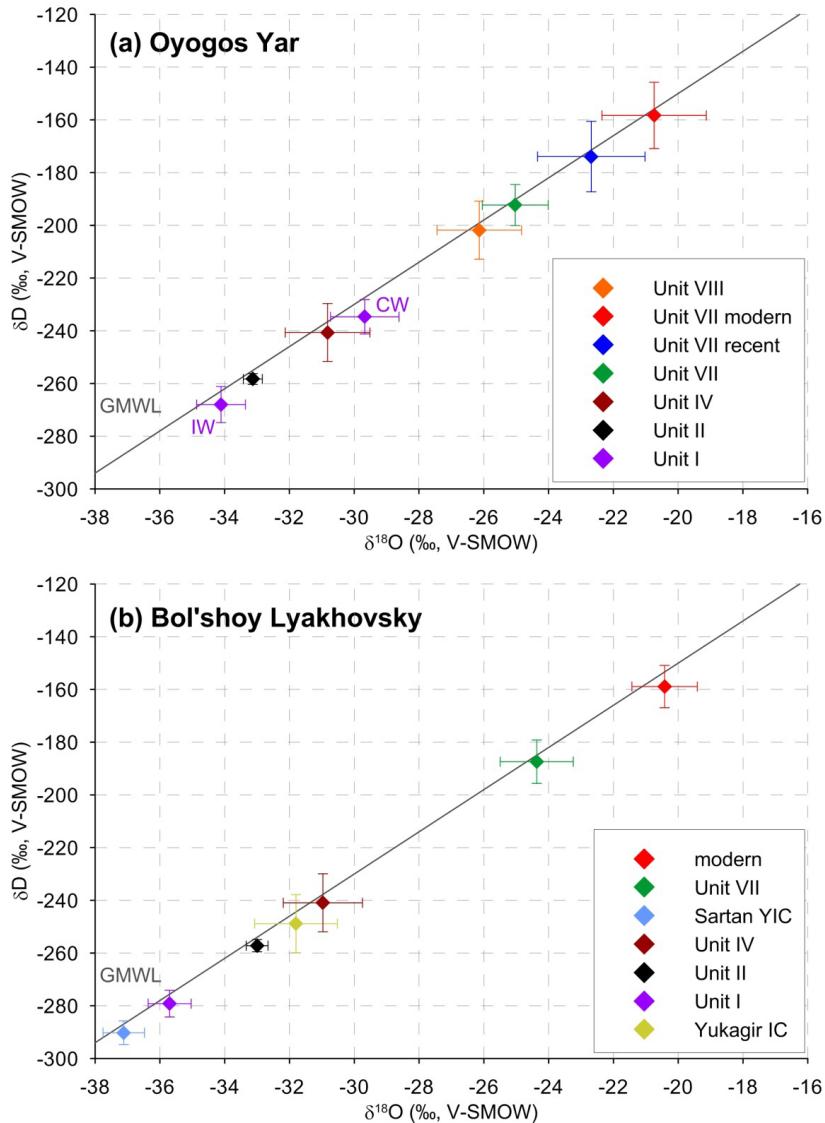
Figure 6. δ¹⁸O-δD diagrams for ice-wedge data of the different units from Oyogos Yar (this study) compared to that from Bol'shoy Lyakhovsky Island (Meyer et al., 2002b; Wetterich et al., 2009; Wetterich et al., 2011; Wetterich et al., 2014; Wetterich et al., 2016). Shown are mean δ¹⁸O and δD values and respective standard deviations. IW indicates ice-wedge samples and CW composite-wedge samples
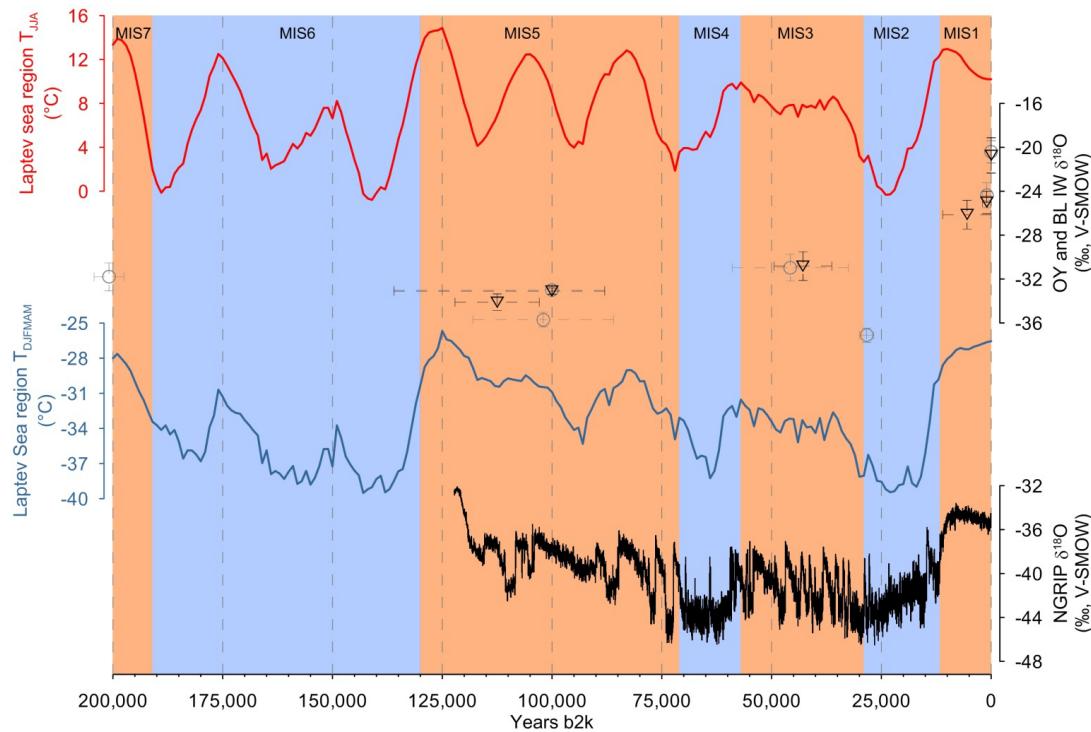
Figure 7. Mean $\delta^{18}O$ data and standard deviations for the different units from Oyogos Yar (triangles) and Bol'shoy Lyakhovsky Island (open circles) (interpreted age with dating uncertainties) compared to modelled summer and winter temperatures for the Laptev Sea region (Ganopolski and Calov, 2011) as well as the NGRIP $\delta^{18}O$ ice core record from Greenland (North Greenland Ice Core Project members, 2004; Wolff et al., 2010).